



HAL
open science

A new hybrid immunocapture bioassay with improved reproducibility to measure tissue factor-dependent procoagulant activity of microvesicles from body fluids

Corentin Franco, Romaric Lacroix, Loris Vallier, Coralie Judicone, Tarik Bouriche, Sophie Laroumagne, Philippe Astoul, Francoise Dignat-George, Philippe Poncelet

► To cite this version:

Corentin Franco, Romaric Lacroix, Loris Vallier, Coralie Judicone, Tarik Bouriche, et al.. A new hybrid immunocapture bioassay with improved reproducibility to measure tissue factor-dependent procoagulant activity of microvesicles from body fluids. *Thrombosis Research*, 2020, 196, pp.414-424. 10.1016/j.thromres.2020.09.020 . hal-03155438

HAL Id: hal-03155438

<https://hal.inrae.fr/hal-03155438>

Submitted on 17 Oct 2022

HAL is a multi-disciplinary open access archive for the deposit and dissemination of scientific research documents, whether they are published or not. The documents may come from teaching and research institutions in France or abroad, or from public or private research centers.

L'archive ouverte pluridisciplinaire **HAL**, est destinée au dépôt et à la diffusion de documents scientifiques de niveau recherche, publiés ou non, émanant des établissements d'enseignement et de recherche français ou étrangers, des laboratoires publics ou privés.



Distributed under a Creative Commons Attribution - NonCommercial 4.0 International License

1 A new hybrid immunocapture bioassay with improved
2 reproducibility to measure tissue factor-dependent
3 procoagulant activity of microvesicles from body fluids

4 Corentin Franco^{1,4} (Corentin.franco@biocytex.fr), Romaric Lacroix^{1,2} (Romaric.lacroix@univ-amu.fr),
5 Loris Vallier^{1,2} (Loris.vallier@gmail.com), Coralie Judicone⁴ (Coralie.judicone@biocytex.fr), Tarik
6 Bouriche⁴ (Tarik.bouriche@biocytex.fr), Sophie Laroumagne³ (Sophie.LAROUMAGNE@mail.ap-hm.fr),
7 Philippe Astoul³ (Philippe.astoul@ap-hm.fr), Françoise dignat-george^{1,2} ([amu.fr](mailto:francoise.dignat-george@univ-
8 amu.fr)), Philippe Poncelet⁴ (Philippe.poncelet@biocytex.fr).

9
10 **Authors' information:**

11 1 Aix-Marseille Université, C2VN, UMR-1263, INSERM, INRA 1260, UFR de
12 Pharmacie, Marseille, France.

13 2 Department of Hematology and Vascular Biology, CHU La Conception, APHM,
14 Marseille, France.

15 3 Division of Thoracic Oncology, Pleural Diseases, and Interventional Pulmonology,
16 Hôpital Nord, AP-HM, Marseille, France.

17 4 Research and Technology Department, BioCytex, Marseille, France.

18
19 **Corresponding author: Prof. Françoise Dignat-George**

20 C2VN, UMR-1263, INRA-1260, Faculté de Pharmacie, 27 Bd Jean Moulin, 13010 Marseille,
21 France. E-mail address: francoise.dignat-george@univ-amu.fr.

22 Abstract

23

24 Background

25 The procoagulant activity of tissue factor-bearing microvesicles (MV-TF) has been associated
26 with the risk of developing venous thrombosis in cancer patients. However, MV-TF assays
27 are limited either by i) a lack of specificity, ii) a low sensitivity, or iii) a lack of repeatability
28 when high-speed centrifugation (HS-C) is used to isolate MV. Therefore, our objective was to
29 develop a new hybrid “capture-bioassay” with improved reproducibility combining MV
30 immunocapture from biofluids and measurement of their TF activity.

31 Materials and Methods

32 Factor Xa generation and flow cytometry assays were used to evaluate IMS beads
33 performance, and to select the most effective capture antibodies. The analytical performance
34 between IMS-based and HS-C-based assays were evaluated with various models of plasma
35 samples (from LPS-activated blood, spiked with tumoral MV, or with saliva MV) and
36 different biofluids (buffer, plasma, saliva, and pleural fluid).

37 Results

38 Combining both CD29 and CD59 antibodies on IMS beads was as efficient as HS-C to isolate
39 plasmatic PS+MV. The IMS-based strategy gave significantly higher levels of MV-TF
40 activity than HS-C in tumor MV spiked buffer, and both pleural fluids and saliva samples.
41 Surprisingly, lower TF values were measured in plasma due to TFPI (TF pathway inhibitor)
42 non-specifically adsorbed onto beads. This was overcome by adding a TFPI-blocking
43 antibody. After optimization, the new IMS-based assay significantly improved reproducibility
44 of MV-TF bioassay versus the HS-C-based assay without losing specificity and sensitivity. In
45 addition, this approach could identify the cellular origin of MV-TF in various biological
46 fluids.

47 Conclusion

48 Compared to HS-C, the IMS-based measurement of MV-TF activity in body fluids improves
49 reproducibility and makes the assay compatible with clinical practice. It can facilitate future
50 automation.

51

52 KEY WORDS

53 Extracellular vesicle, Functional assay, Immunocapture, Microvesicle, Reproducibility,
54 Tissue factor

55

56

57

58

59 INTRODUCTION

60

61 Stratification of patients according to their thrombotic risk remains a real challenge in various
62 clinical settings such as cancer, cardiovascular disease, and immuno-inflammatory diseases.
63 Current combinations of clinical and biological variables still fail to efficiently predict the risk
64 of thrombosis arguing for a need for predictive biomarkers. Among the candidates, large
65 extracellular vesicles (better known as microparticles or microvesicles, MV) are present in all
66 biological fluids (blood, saliva, pleural effusions, etc.). They can promote coagulation and
67 thrombosis (1–4). Indeed, MV provide a catalytic surface for the assembly of the coagulation
68 complexes through 1) the exposure of anionic phospholipids such as phosphatidylserine (PS)
69 on the external leaflet of the membrane and 2) the presence of tissue factor (TF), which is the
70 main initiator of the coagulation cascade, on some subsets of vesicles (5–8).

71 The contribution of TF+ large extracellular vesicles (MV-TF) in thrombus formation (9–12)
72 has been demonstrated in animal models using injection of exogenous MV from either
73 leukocytes, endothelial cells, or tumor cells; it may also use endogenous production of cancer-
74 derived MV. Moreover, prospective studies in cancer patients showed an association between
75 elevated levels of MV-TF and the risk of developing venous thrombosis. However, the
76 association between high levels of MV-TF and VTE has been shown in tumors with a high
77 risk of thrombosis such as in glioblastoma and pancreaticobiliary cancer (13–16). This may be

78 due to a lack of sensitivity and reproducibility of the current methods used to measure MV-TF
79 in clinical samples as well as heterogeneous mechanisms involved in thrombus formation
80 according to the type of cancer and the cellular origin of the MV (17).

81 Assays currently available to measure MV-TF are based on different approaches—either
82 detecting the TF antigen on MV or measuring the TF-dependent procoagulant activity of MV.
83 Antigenic detection of TF on circulating MV shows limitations because 1) both cryptic and
84 decrypted TF may be equally detected whereas these two forms are not equally active and 2)
85 the measurement of TF by flow cytometry remains challenging because of its low levels on
86 MV (18,19). Alternative methods evaluate TF activity by measuring the capacity of MV to
87 generate factor Xa, thrombin, or a clot (20–23). In order to tackle specificity and sensitivity
88 issues related to such functional assays, we recently developed a new MV-TF activity assay
89 that includes a specific control based on an inhibitory anti-TF antibody (SBTF1) and involves
90 an optimized protocol (24) with improved specificity. However, the isolation process remains
91 a critical step. Indeed, when high-speed centrifugation (HS-C) is used for the isolation of MV
92 from plasma samples, variable activity levels are obtained with different rotors despite
93 standardization of the centrifugation protocol (time, speed, ...); this leads to a lack of
94 reproducibility (24). Moreover, HS-C is known to generate MV aggregates impeding further
95 delineation of the cellular origin of the TF activity (25).

96 Beside this technical issue impeding the reproducibility of TF dependent MV assays, another
97 limiting condition is that none of them identify the cellular origin of MV-TF. The interest to
98 focus on specific subsets of MV-TF activity is supported by 1) the selective expression of TF
99 on endothelial, leukocytic, or tumor cell-derived MV and 2) the potential better predictive
100 value of MV subsets in regard to disease severity and cardiovascular complications(26).

101 Therefore, our objective was to develop a new assay, independent from HS-C, to improve the

102 repeatability of the current HS-C based assay (without losing specificity and sensitivity).
103 Thus, immunomagnetic separation (IMS) was chosen as the MV isolation method. Our study
104 shows that IMS offers efficient, repeatable, and selective measurement of MV-TF activity in
105 various human body fluids (plasma, saliva, and pleural fluids).

106 MATERIALS AND METHODS

107

108 Biological fluid collection

109

110 Platelet-free plasma

111 Platelet-free plasma (PFP) were prepared from local blood bank donors, who signed an
112 informed consent, being collected and processed according to the current minimal information
113 for studies of extracellular vesicles guidelines(27). Briefly, blood was collected into 2.7 mL
114 Vacutainer® tubes containing 0.109 mol/L sodium citrate (BD Diagnostics, Rungis, France)
115 and incubated w/o lipopolysaccharide (LPS) (1 µg/mL, Escherichia coli O111: B4; Sigma
116 Aldrich, Lyon, France) for 10 h at RT. The PFP was prepared with two successive
117 centrifugations (2,500 g, 15 min, RT with a 5417R or C centrifuge -Rotor: F-45-30-11,
118 Eppendorf, Montesson, France) and stored at -80°C until use.

119 Pleural fluids

120 Pleural effusion samples from cancer patients had been collected and processed as previously
121 published(28). Briefly, they were centrifuged at 300 g for 10 min and at 1,000 g for 15 min at
122 room temperature without stopping. The collected supernatant was stored at -80°C until
123 further use. After thawing in a water bath at 37°C, a 1:10 dilution was necessary before
124 measuring the MV-TF activity.

125 Saliva

126 Saliva samples (5 ml) were collected from healthy donors who did not eat or brush their teeth
127 at least two hours before sampling. Samples were diluted 1:10 in buffer H (150 mM NaCl, 20

128 mM HEPES (4-(2-hydroxyethyl)-1-piperazine ethanesulfonic acid) and 0.1% NaN₃, pH 7.4,
129 0.22 µm filtrated) and centrifuged twice at 2500 g (15 min without a break) to remove cell
130 debris before storage at -80°C until use. After thawing in a water bath at 37°C, an initial
131 dilution of 1:3 was necessary before measuring MV-TF activity or for spiking experiments.

132

133 [BxPC-3 and HAP-1 microvesicles preparation](#)

134 Human adeno-pancreatic BxPC3 cells (Sigma Aldrich, Lyon, France) were cultured in RPMI
135 1640 medium (Thermo Fisher Scientific, Illkirch-Graffenstaden, France) supplemented with
136 10% fetal bovine serum (FBS), 1% penicillin, and 1% streptomycin (GIBCO BRL) in a
137 humidified atmosphere at 37 C, 5% CO₂. Haploid human cell line (HAP1) and its TF knock-
138 out derivative KO-TF-HAP1 were grown at 37°C and 5% CO₂ in Iscove's Modified
139 Dulbecco's Medium (IMDM) supplemented with 10% FBS, 1% penicillin, and 1%
140 streptomycin. Cell viability was assessed by trypan blue dye exclusion. TF-protein expression
141 was checked by flow cytometry, and TF-gene expression was checked by qPCR. Cells were
142 diluted 1:4 in new medium when they reached 80% confluence. The MV rich culture
143 supernatant was cleared from cells by two successive centrifugations at 300 g for 5 min and
144 from debris by centrifugation at 2,500 g for 15 min. Finally, MV were pelleted by HS-C at
145 24,000 g, 60 min, and washed twice in PBS-BSA ([PBS BSA 0.1% - sodium azide 0.09%](#))
146 before storage at -80°C until use. After thawing, MV were enumerated by flow cytometry as
147 detailed below and spiked either in PFP or HEPES buffer.

148 [Immunomagnetic beads preparation](#)

149

150 [Streptavidin beads selection](#)

151 Streptavidin paramagnetic beads were selected according to the following criteria: a) a
152 nominal size of 1 µm, b) a low non-specific capture of proteins, c) the absence of detergent in
153 the final storage and reaction buffer, and d) a high level of free biotin binding per unit.

154

155 [Antibody biotinylation](#)

156 Many antibodies were used: CD4, CD11b, CD11c, CD13, CD14, CD15, CD18, CD24, CD29,
157 CD30, CD33, CD38, CD41, CD43, CD45, CD45 RA, CD45 RO, CD46, CD48, CD52, CD54,
158 CD55, CD59, CD61, CD62P, CD62L, CD63, CD64, CD66B, CD68, CD81, CD85j, CD86,
159 CD89, CD98, CD99, CD101, CD115, CD131, CD146, CD162, CD326, anti-HLA-DR, and
160 the irrelevant IgG1 control anti-DNP (Dinitrophenol). These were provided by Biocytex after
161 being labeled as follows: antibodies were mixed with Sulfo-NHS-LC-Biotin (EZ-
162 link/ThermoFischer, Illkirch-Graffenstaden, France) in amine-free PBS for 30 min at RT.
163 Biotin-labeled antibodies and free biotin were separated using a desalting column in PBS
164 (Sephadex G-25 in PD-10, GE Healthcare/Life Sciences, Tremblay-en-France, France).
165 Positive fractions were concentrated with Amicon® Ultra-4 (Merck, Darmstadt, Deutschland)
166 to obtain a final concentration of antibody higher than 1 mg/ml. Finally, biotinylated
167 antibodies were stored in a conservation buffer at 4°C (PBS-Azide; 0.137 M NaCl, 0.27 mM
168 KCl, 0.01 M Na₂HPO₄ 18 mM KH₂PO₄, 0.09% sodium azide, pH: 7.4).

169 [Coating and storage of streptavidin beads](#)

170 Before coating, streptavidin beads were washed in PBS-BSA using a magnet bead separator
171 (Dynamag-2, Invitrogen Dynal, Oslo, Norway). The beads were then incubated with the
172 antibody solution during one min at RT. After removal of the supernatant, antibody-coated
173 beads (IMS-beads) were washed in PBS-BSA buffer and stored at 4 mg/ml in the same buffer
174 at 4°C.

175

176 [IMS-based MV-TF activity assay](#)

177 MV-TF activity was measured in samples either after isolation by HS-C as previously
178 published (24) or by IMS as follows. Briefly, 100 µL of sample were incubated for 60 min at
179 RT under mild rotative mixing. Different conditions of bead amount and contact time with

180 MV were tested as reported in the results section. The MV-loaded beads were washed and
181 resuspended in 140 μ l of HEPES buffer. The TF activity was then measured by a fluorogenic
182 assay as described in Vallier et al. (24). Briefly, aliquots (70 μ l) were pre-incubated for 30
183 min at 37°C with either an inhibitory anti-TF monoclonal antibody (10 μ g/ml final, clone
184 SBTF-1, BioCytex, Marseille, France) or a control antibody (10 μ g/ml, clone a-DNP 2H11-
185 2H12, BioCytex, Marseille, France). Then, 8 μ l HEPES-Ca²⁺ buffer (150 mM NaCl, 20 mM
186 HEPES and 0.1% NaN₃, 50 mM CaCl₂, pH 7.4, 0.22 μ m filtrated) containing purified human
187 FVII and FX (Stago BNL, JV Leiden, Netherland) was added to each 70 μ l sample to produce
188 final concentrations of 10 nM, 190 nM, and 5 mM CaCl₂ respectively and incubated for
189 another 2 h at 37°C. FXa generation was stopped by the addition of 8 μ l of EDTA buffer (150
190 mM NaCl, 20 mM HEPES and 0.1% NaN₃, 200 mM EDTA, pH 7.4, 0.22 μ m filtrated). To
191 avoid beads interference, the supernatant was transferred in another plate after magnetization
192 of beads. The FXa fluorogenic substrate (1 mM final, BioCytex, Marseille, France) was added
193 onto the bead supernatant. Finally, the fluorescence at 390 nm (excitation) and 460 nm
194 (emission) was monitored for 15 min at 37°C on a microplate fluorescence reader
195 (Fluoroskan, CAT instrument, Stago, Asnières-sur-Seine, France). Data from plasma-purified
196 MV were expressed as fmol/L by comparison to a calibration curve generated using
197 recombinant TF. Irrelevant IMS were performed using beads coated with an antibody against
198 DNP—a small hapten molecule not expressed on human cells.

199

200 Flow cytometry analysis

201

202 Microvesicle gating

203 MV were analyzed by flow cytometry on a last generation instrument (CytoFLEX S*,
204 Beckman Coulter) in which the side scatter (SSC) parameter was collected at 405 nm (violet
205 SSC) to improve the size-related resolution in the sub-micron range. A standardized gate for

206 MV analysis was determined with the help of a new tool called Gigamix-Plus (BioCytex)
207 made of eight different polystyrene beads (75 nm, 100 nm, 160 nm, 200 nm, 240 nm, 300
208 nm, 500 nm and 900 nm) obtained by mixing both Megamix-Plus SSC and FSC beads (29),
209 and supplementing by an additional 75 nm bead. We set the MV gate using Gigamix-Plus in
210 comparison to Megamix-Plus SSC as described in detail in Supplemental Figure 1. Briefly,
211 the lower limit is defined under the 75 nm beads and the upper limit is over the 900 nm beads.

212

213 [Microvesicle enumeration](#)

214 Samples (10 μ l) containing MV were incubated 15 min at RT with a mixture of 0.7 μ l of
215 Annexin V-FITC (fluorescein isothiocyanate) 1:30 in calcium buffer (Tau Technology,
216 Kattendijke, NL), 0.7 μ l CD235a-AF735 (Alexa Fluor735, 11E4B-7-6, Beckman-Coulter),
217 0.7 μ l CD15-BV650 (brilliant violet 650, W6D3, Biolegend Saint-Cyr-l'École, France), and
218 0.5 μ l CD41-PE (phycoerythrin, PL2-49, Biocytex) or 0.5 μ l of HLA DR-PE (Immu-357,
219 Beckman Coulter) in 100 μ l calcium buffer. The positivity threshold was determined
220 beforehand with isotype controls matched with their relevant antibody conjugates in terms of
221 fluorescence background. The MV subsets were defined as follows: platelet-MV (PMV) as
222 AnnV+/CD41+, erythrocyte-MV (EryMV) as AnnV+/CD235a+, granulocyte-MV (GranMV)
223 as AnnV+/CD15+, monocytes-MV (and few B lymphocytes-MV) (HLA-DR MV) as
224 AnnV+/HLA-DR+, and epithelial cancer MV as AnnV+/CD326+. When needed, absolute
225 counts of MV were determined using MP-Count Beads (BioCytex) as previously published
226 (30).

227

228 [Statistical analysis](#)

229 Statistical analyses were performed with GraphPad Prism software version 5.0 (GraphPad
230 Software, San Diego, CA, US). Significant differences were determined using a non-

231 parametric Mann-Whitney test and one-way ANOVA. A p-value less than 0.05 was
232 considered statistically significant.

233

234 RESULTS

235

236 Comparison of IMS and high-speed centrifugation to isolate MV from plasma

237

238 To select the best immuno-magnetic tools to isolate MV from body fluids, we first evaluated
239 the MV capture efficiency of several magnetic beads coated with various antibodies. This was
240 achieved by counting the remaining MV detectable by flow cytometry in plasma samples
241 post-IMS. Figure 1A illustrates a few examples of isolations by beads coated with antibodies
242 against CD55, CD15, CD41, and anti-HLA-DR. Either all PS+ MV (AnnV+ MV) or the
243 specifically targeted subsets Gran-MV (CD15+), PMV (CD41+) or Mono- (+/- B
244 Lymphocytes, HLA-DR+) MV were removed.

245 The performance of IMS in depleting MV from various subtypes is reported in Table 1. Non-
246 specific depletion with Ctrl-IMS was minimal (<5%). IMS-based MV isolation depended on
247 the beads' specificity. Lineage-oriented magnetic separations were efficient to remove their
248 respective targets: CD41-coated beads removed 98+/-3% of PMV, CD15 beads removed
249 92+/-4% of Gran-MV, and anti-HLA-DR-coated beads removed 84+/-15% of Mono-MV. The
250 non-specific capture induced by unreactive beads (a-DNP IMS) remained low (< 5%). The
251 non-specific capture of untargeted MV subsets in lineage-oriented IMS systems was
252 sometimes surprisingly higher than expected (up-to 35%) and was mainly observed when the
253 most frequent PMV subset was targeted using CD41 IMS. In our hypothesis, the highest
254 levels of non-specific capture might be due to the co-isolation of aggregated vesicles, e.g.,
255 CD15+ Gran-MV aggregated with CD41+ PMV may come out with CD41 IMS.

256 However, each of these individual bead types captured significantly less FCM-characterized
257 PS-expressing MV (AnnV+ MV) than what HS-C could isolate. Therefore, these could not
258 replace HS-C for exhaustive capture. Even beads targeting widely represented antigens
259 (CD29, CD55, CD59, and HLA-ABC) provided a significantly lower percentage of isolation
260 than HS-C. Thus, a combination strategy was tested where the same beads were coated with
261 two different antibodies with synergistic antigenic coverage (CD29-59 IMS). Figure 1B and
262 Table 1 show that CD29-59 IMS could isolate as many AnnV-MV as HS-C (84+/-7% vs
263 82+/-10%, respectively, $p = 0.7$). CD29-59 IMS and HS-C displayed the same efficiency to
264 isolate CD41, CD15, and HLA DR MV from plasma and was significantly more efficient to
265 capture the CD235a+ (erythrocytic) MV. The CD29-59 beads were therefore selected as an
266 appropriate tool to replace centrifugation.

267 [Comparison of CD29-59 IMS and high-speed centrifugation based MV-TF activity](#) 268 [assays in different body fluids](#)

269 The efficacy of CD29-59 IMS to isolate the MV-TF activity was tested on different body
270 fluids, by reference to HS-C. Figure 2A shows that when using CD29-59 IMS rather than HS-
271 C, TF activity levels were significantly increased for saliva (+53% +/-5.3%, $p=0.007$) and for
272 tumoral pleural effusions (+84 +/-4.7%, $p=0.016$). Similarly, significantly more MV-TF
273 activity was measured when tumoral MV (BxPC3 MV) was spiked in HEPES buffer.
274 However, the IMS-based activity dropped when the same amount of MV was spiked in
275 plasma suggesting that a soluble plasma component interfered with this measurement. Thus,
276 we tested the hypothesis that TFPI (tissue factor pathway inhibitor: the major plasmatic
277 inhibitor of TF) may be adsorbed on the plastic beads rather than be washed-out after IMS. A
278 range of TFPI concentrations (0-1500 ng) was incubated on unspecific IMS beads (Ctrl-IMS)
279 in HEPES buffer. After 60 minutes, Ctrl IMS beads were washed and incubated with BxPC-3
280 MV. As a result, we observed a dose-dependent inhibition of the MV-TF activity starting
281 from the infra-physiological [TFPI concentration of 6.2 ng/ml](#) (Figure 2B).

282 As confirmed in Figure 2C, the MV-TF activity was inhibited when IMS beads were pre-
283 incubated in normal plasma (NP) but was preserved using TFPI-deficient plasma (DEF) or in
284 the presence of an anti-TFPI antibody. Altogether, these results demonstrate that plasmatic
285 TFPI is adsorbed by the IMS beads and is responsible for the decrease of MV-TF activity
286 isolated from plasma. Therefore, the anti-TFPI antibody was systematically incorporated into
287 the IMS-based assay, and also into the HS-C-based assay for future comparisons.

288

289 Optimization of IMS conditions for measuring MV-TF activity.

290

291 To optimize the IMS conditions, we next varied the concentration of beads and the time of
292 MV capture. MV-TF activity was measured in plasma samples prepared from LPS-treated
293 whole blood. Figure 3A shows that a minimum amount of 3N (N=33 μ g) CD29-59 beads was
294 required to get significantly increased MV-TF activity versus HS-C (+33% +/-3%, p =
295 0.0132). No significant increase was found upon further increasing the amount of beads; thus,
296 3N was selected as the adequate quantity. Using this amount of beads, we next defined the
297 optimal time of capture to be 60 min (Figure 3B). Interestingly, increasing the amount of
298 beads (6N) could reduce this time down to 30 min. However, the condition 3N x 60 min was
299 selected as the best compromise between cost and IMS-based isolation efficiency for further
300 experiments. These chosen IMS conditions were robust to the amount of total MV present in
301 the sample. Indeed, as illustrated in Suppl Fig. 2, the MV-TF activity could be efficiently
302 isolated even in a large excess of total MV in the sample after spiking LPS-activated plasma
303 with MV from saliva and increasing the total load of MV more than 10-fold.

304 Of note, these same IMS conditions were also verified to deplete more than 95% of the TF
305 antigen present in a suspension of washed BxPC3 MV as illustrated in Suppl. Fig. 3; HS-C
306 still left about 10% of MV-associated TF in the supernatant.

307

308 [Evaluation of analytical performance of the IMS-based MV-TF activity assay](#)

309

310 We then evaluated the sensitivity, specificity, linearity and reproducibility of the optimized
311 IMS assay in various models of platelet-free plasma. First, in the BxPC3 MV-spiked plasma
312 model, we showed that TF-PCA was significantly increased using IMS versus HS-C (67+/-
313 4.0 fM vs 13+/-7.0 fM; $p < 0.0001$, $n = 9$; Figure 4A). This increased sensitivity was confirmed
314 while studying the other model of plasma from LPS-activated versus unstimulated blood
315 (Figure 4B), even in the lower range of MV-TF concentrations measured in normal plasma
316 (10+/-1.3 fM vs. 4.0+/-2.7 fM; $p = 0.002$). Second, the TF specificity of the IMS-based assay
317 was checked using MV (HAP-MV), which had TF knocked-out. Figure 4C shows that no TF-
318 specific activity was measured over a wide range of concentrations of KO-TF-HAP MV in
319 contrast to parental MV (HAP-MV), confirming the specificity of the assay. Third, the test
320 had good linearity using the same MV ($r^2 > 0.99$; Figure 4D).

321 [The quantity of IMS beads used in our MV isolation protocol should not only be optimal for](#)
322 [normal plasma but should also be applicable in a pathological context associated with high](#)
323 [amounts of MV. This was checked with a model of plasma spiked with excess amounts of](#)
324 [saliva MV. Indeed, our system maintained a comparable MV isolation capacity despite the](#)
325 [addition of more than 10 times the amount of total MV present in unspiked plasma.](#)
326 [\(Supplemental Figure 2\).](#)

327 Finally, we compared IMS and HS-C (Table 2) in terms of reproducibility. The coefficient of
328 variation (CV) for repeated assays was lower using IMS than HS-C in low, medium, and high
329 ranges of activity (mean value: 9% +/-5% vs 25% +/-10%, $p = 0.05$). Similarly, the inter-
330 operator reproducibility was significantly improved in the IMS condition (CV mean value:
331 12% +/- 5.5% vs 28% +/- 11%, $p = 0.04$). These results showed the better reproducibility of the
332 CD29-59 IMS-based MV-TF activity assay versus the HS-C-based version without losing the
333 sensitivity and TF specificity of the assay.

334

335 Identification of the origin of MV-TF by selective IMS

336

337 One theoretical advantage of immunological capture is to help identify the cellular origin of
338 MV-TF. Thus, we performed multiple selective IMS made to capture MV subsets on plasma
339 from LPS-activated blood (LPS-plasma) and cancer pleural fluids. A case of LPS-plasma is
340 illustrated in Figure 5A featuring an initial screening of forty putative target antigens
341 including platelet-, endothelium- and leucocyte-associated markers; mostly monocyte-
342 associated markers were chosen here because of the well-known TF-inducing effect of LPS
343 activation on monocytes.

344 IMS experiments were stratified according to the level of isolated TF activity. Figure 5A
345 shows a broad range of TF activity levels depending on the specificity of the antibody coated
346 on the IMS beads. IMS isolations with an activity <5 fM TF were considered negative
347 including those targeting the platelet-, endothelium-, and granulocyte-lineage specific
348 antigens CD41, CD61, CD62P, CD146, and CD66b. In contrast, some IMS beads were
349 isolated with high activity levels (\sim or > 50 fM), which is comparable to that of our previous
350 “Pan MV” reference CD29-59 IMS, i.e., CD11b, CD18, anti-HLA-DR, CD33, and CD45.
351 Interestingly, most other IMS beads tested, targeting well-known monocyte-associated
352 antigens such as CD14, CD64, CD11c, CD13, CD38, CD4, CD54, and CD162, collected
353 lower albeit clearly significant levels of activity (10-50 fM TF). This suggests a monocytic
354 origin of the TF-PCA in this sample (Fig. 5A).

355 A new experiment (Fig. 5B) clearly confirmed this preferential monocytic orientation. Other
356 than the anti-HLA-DR IMS that recovered the same high level of activity as the “pan-MV”
357 CD29/59 IMS, the gran-MV-oriented CD15 IMS, the PMV-oriented CD41 IMS, and the
358 endo-MV-oriented CD146 IMS all captured negligible levels of TF activity.

359 We similarly studied the MV-TF activity in the case of cancer pleural effusion (Fig. 5C). This
360 was mainly supported by MV showing the positivity for CD326, i.e., the epithelial cell
361 adhesion molecule (EpCAM)—an antigen over-expressed on most solid tumors. In addition to
362 CD326 IMS, significant levels of TF-PCA were also isolated from this single example of
363 pleural fluid using anti-HLA-DR as well as CD146 IMS suggesting the presence of
364 TF+/HLA-DR+ monocyte MV (MonoMV) as well as TF+/CD146+ Endo-MV or the co-
365 expression of these antigens (EpCAM/CD326, HLA-DR and MCAM/CD146) on the same
366 Tumor-MV. Thus, IMS allowed the use of a large library of specificities and was a useful tool
367 to investigate the cellular origin of the MV-TF activity in biological samples.

368

369 DISCUSSION

370

371 Here, we developed a new hybrid capture bioassay to measure MV-TF activity that bypasses
372 HS-C to isolate MV from human body fluids. The novelty of this assay is that it combines the
373 specific immunocapture of MV from body fluids with the measurement of TF activity. The
374 use of magnetic beads coated with both anti-CD29 and anti-CD59 antibodies is as efficient as
375 HS-C to isolate all PS+ MV detectable by flow cytometry. It is more efficient than HS-C to
376 recover the MV-associated TF activity. The use of several body fluids (plasma, pleural fluid,
377 and saliva) demonstrated that the new assay was more reproducible than the HS-C-based
378 assay without losing sensitivity and TF specificity. Moreover, we showed for the first time
379 that IMS can identify the cellular origin of MV-TF in biological samples.

380 Whole plasma (or even whole blood) coagulation assays have been proposed to measure TF-
381 dependent procoagulant activity (TF-PCA)(8,31,32). Although each of the TF activity assay
382 principles has its own advantages and limitations, global assays are most often dependent on

383 inhibitors such as TFPI, clotting factors other than TF, or on-going treatments(33) such as
384 heparin(32) or oral anti-coagulants. Such assays are also affected by non-TF-dependent
385 alternative coagulation systems such as the contact pathway. These assay principles may need
386 blockage with CTI or anti-FXI antibodies(31,32) to neutralize the contribution of the contact
387 pathway and they often create complex result interpretation.

388 In contrast, our approach avoids interferences by first isolating TF-bearing MV from their
389 plasmatic environment and then using synthetic systems to reveal TF activity as already
390 described for FXa generation assays. Indeed, most whole plasma methods such as the fibrin
391 generation test(32) also use MV isolated from patient samples followed by spiking into a
392 well-known matrix of MV-free normal plasma pool. Thus, even with whole plasma or blood
393 clotting assays, MV isolation prior to TF-PCA evaluation looks like a mandatory step as
394 shown by Aras et al(34).

395 Different methods have been described in the literature to isolate small or large extracellular
396 vesicles (EV) from various biological fluids (35,36). Among methods based on physical
397 properties of MV, density gradient separation and especially flotation result in a good purity
398 of EV but are very time-consuming with generally low and non-reproducible yields (37,38).
399 Polymer-based isolation mainly including poly-ethylene glycol (PEG) precipitation is fast but
400 shows a high level of non-EV contamination (37,38). Size exclusion chromatography (SEC)
401 is a good compromise between yield and purity but necessitates sample re-concentration after
402 elution and is not compatible with clinical practice (39,40). Centrifugation, either “high-
403 speed” (HS-C i.e. ~20,000 g) for large EV (MV) or ultra-centrifugation (> 70,000 g) for small
404 EV is the most commonly used method for isolating EV; however, centrifugation is time-
405 consuming and provides EV with low recovery, low purity (41–43) and limited reproducibility
406 (24). Immunological approaches based on target antigen(s) expression can use FACS to
407 specifically isolate large EV, but this is time-consuming and requires expensive and

408 complex equipment (44). Microfluidic techniques (45) based on immuno-capture of EV in
409 micro-channels can be specific, but they may also be characterized by low recovery yields due
410 to a limited binding capacity.

411 By illustrating IMS in biological fluids other than plasma samples, we demonstrate here that
412 this new approach 1) can be applied in various body fluids regardless of the viscosity of the
413 medium and 2) that its efficacy is as good as high speed centrifugation (HS-C). Indeed, media
414 viscosity is a critical parameter that influences the efficiency of EV isolation for most EV
415 isolation techniques. Importantly, IMS may be one of the least influenced isolation methods
416 because affinity binding rather than physical properties of EVs are the main drivers. Indeed,
417 IMS as an isolation technology for e.g. cells or bacteria, has been applied in complex
418 biological samples such as whole blood, bone marrow, and even stool samples. Thus, it
419 appears to be the most appropriate for viscous media.

420 We showed here that the new IMS strategy was as efficient as HSC to isolate MV. Indeed, the
421 use of magnetic beads coated with antibodies with broad specificity allows exhaustive capture
422 of target antigen-positive MV probably due to the large binding surface provided by
423 microspheres ensuring high probability of meeting between MV and beads. IMS has already
424 been used to isolate either i) most EV via targeting broadly represented molecules or ii)
425 subsets of EV using lineage-specific antigens. First, phosphatidylserine (PS) was targeted to
426 isolate EV using beads coated with annexin V or TIM-4 (T-cell membrane protein 4) in a
427 calcium-dependent manner or with lactadherin (46,47) as a calcium-independent alternative.
428 However, PS is not expressed on all EV (48). Tetraspanins (CD9, CD63, and CD81) are the
429 most frequently targeted antigen to isolate EV (49) but these specificities are mostly related to
430 small EV and may not cover all EV especially the procoagulant TF-positive MV that we aim
431 to collect. We used a screening strategy based on numerous cell-surface CD to show that the
432 combined targeting of both CD29 and CD59 antigens was an effective strategy to isolate most

433 MV in general as seen in FCM and most TF activity-bearing MV in particular. This potential
434 was probably due to their broad and complementary expression on circulating cells and also
435 MV. Indeed, CD59/MIRL serves as a complement decay ecto-enzyme and must be present on
436 all nucleated cells as well as on red blood cells at a significant level (e.g. 45,000
437 molecules/RBC (50)) since its absence is pathological, e.g. in paroxysmal nocturnal
438 hemoglobinuria (51). We also considered this to be an attractive target since its GPI
439 anchorage appears favorable for its association with lipid rafts and thus its incorporation onto
440 EV membrane (52,53). Integrins are also known to be well expressed on MV (54) and
441 CD29—these are common beta chains of all very late activating antigen (VLA; CD49 a to f)
442 and can be found on many leucocytes. This glycoprotein is also present on platelets as part of
443 the GPIa/IIa complex; thus, it complements the low expression of CD59 on platelet (and
444 PMV) surfaces.

445 Compared to HS-C, our IMS strategy was more sensitive to recovering the MV-associated TF
446 activity. Indeed, the MV-PCA was higher in the IMS assay than the HS-C in tumor MV-
447 spiked buffer, saliva, and pleural fluids. The apparent decrease observed in plasma was due to
448 a nonspecific adsorption of TFPI onto beads—this decrease was overcome by adding a TFPI
449 blocking antibody. The addition of anti-TFPI in thrombin generation assays increases the
450 activity already reported (55). This addition is a major difference with the previous HS-C
451 version of the assay (24) and asks whether the information obtained by the two types of
452 assays is of similar nature given the pathophysiological role of TFPI. However, previous
453 observations questioned the HS-C process around 20,000 g and the subsequent EV washing
454 already removed the soluble TFPI while higher centrifugation speeds (>70,000 g) retained it
455 (24). In agreement with that, the conditions of the HS-C-based MV-TF activity assay (24,000
456 g, 1 h x 2) showed no significant difference with or without the presence of TFPI-neutralizing
457 antibody (data not shown). Thus, both the HS-C and IMS versions of the MV-TF assays

458 measure similar information. Therefore, better sensitivity of the new IMS-based assay in
459 comparable volumes (i.e. 100 μ L) of plasma should be attributed to a better level of MV
460 capture rather than to the inhibition of TFPI because we demonstrated an exhaustive (>95%)
461 immune-depletion of the MV-associated TF antigen whereas HS-C left about 10% in the
462 supernatant (illustrated in Suppl. Fig. 3).

463 This higher sensitivity of CD29-59 IMS versus HS-C was demonstrated by 1) the existence of
464 a basal level of MV-TF activity that was much higher in unstimulated PFP from healthy
465 donors and by 2) the significant increase of activity for MV in LPS-stimulated PFP. The
466 higher sensitivity of the new IMS-based assay is probably due to a better level of MV capture
467 especially the smallest ones that express TF and PS but remain below the detection threshold
468 of the most sensitive flow cytometry protocol.

469 The most important technical advance of our new hybrid TF assay is to bypass HS-C to
470 isolate MV. Indeed, we have previously shown that isolation of the MV by HS-C has limited
471 reproducibility and repeatability as shown by the CV of MV TF activity data: These metrics
472 were significantly improved by bypassing centrifugation (56). This limited reproducibility
473 associated with HS-C is consistent with previous studies showing that the recovery of the
474 pellet depends on the rotor type, the centrifugation speed (g-force), and the centrifugation
475 time (57): These are physical parameters that were shown to significantly affect MV TF
476 activity (56). Other disadvantages of centrifugation are the induction of MV aggregation (36)
477 and the failure to discriminate MV from contaminating structures such as protein/lipid
478 aggregates (35); both of these are responsible for limited purity. Here, we show that the use
479 magnetic beads is an option to overcome the disadvantages of centrifugation and can
480 specifically reducing the time to isolate MV and avoid washing steps.

481 As we first showed in Cointe et al. (58), IMS was more reproducible than HS-C to evaluate

482 the fibrinolytic capacity of CD15 + MV in septic patients (58). This work similarly shows a
483 major improvement brought into this PCA assay, i.e, lower CVs measured for intra-assay
484 repeatability (mean value: 9% +/-5% vs 25% +/-10%, p=0.05; Table 2). Also, the inter-
485 operator reproducibility was significantly improved in the IMS condition (CV mean value:
486 12% +/- 5.5% vs 28% +/- 11%, p=0.04). This reproducibility was not obtained at the expense
487 of sensitivity nor TF specificity. This increase is likely because IMS requires minimal hands-
488 on time and produces purified MV enabling downstream analysis.

489 Although intrinsic assay performance seems encouraging, the clinical interest of this new
490 IMS-based MV-TF activity assay to predict thrombosis remains to be evaluated. The potential
491 of this assay format using IMS for automation on laboratory robots should even enable better
492 robustness for future routine use. Interestingly, it will have value in both plasma and other
493 biofluids.

494 Moreover, we showed that IMS can provide an opportunity to identify the cellular origin of
495 MV-TF in biological samples. We first used a well-known model in the field where in vitro
496 LPS activation of whole blood induces i) de novo TF expression on the surface of monocytes
497 (59) as well as ii) TF PCA in plasma derived from the activated blood. Our study involved a
498 screening strategy with numerous cell-surface targets (CD) including or lineage-specific or
499 lineage-associated antigens (e.g., monocyte-associated antigens). We found that most of these
500 specificities could isolate significant TF activity. This confirmed the expected monocytic
501 origin of MV-TF activity in plasma from LPS-activated blood. The fact that targeting these
502 monocyte-associated markers isolated different levels of activity may be linked to variations
503 in i) antigen density on monocyte-derived TF+EV and ii) monoclonal antibody affinity. In
504 contrast, all IMS isolations directed against antigens specific for other MV subsets were
505 negative including those against Gran-MV (CD15, CD66b), Endo-MV (CD146), and PMV
506 (CD41, CD62P) with CD61 being possibly shared between PMV and EMV(60)

507 The new IMS strategy was also useful to define the cellular origin of MV-PCA in pleural
 508 fluid sample as illustrated for a case of EpCAM-positive epidermoid cancer. Indeed, CD326+
 509 tumor-MV could be detected in this fluid illustrating that specific IMS isolation of EV
 510 included into a bioassay provides useful information to delineate the tumor cell origin of the
 511 MV-TF activity.

512 IMS has been previously used to isolate specific tumoral subsets using glypican-1 (61) to
 513 identify cancer exosomes, EpCAM to detect epithelial cancers (62,63), EGFRv3 to capture
 514 glioblastoma-derived small EV (64), CSPG4 to detect patients with melanoma (65), and CA-
 515 125 to detect ovarian cancer (66). However, none of these IMS-based approaches were
 516 intended to quantify a functional activity on EV.

517 Thus, measuring MV-TF activity using IMS isolation is an innovative approach that tackles
 518 the issue of HS-C reproducibility without losing sensitivity or TF specificity and gives access
 519 to the determination of TF-PCA on MV subpopulations. These crucial improvements make
 520 the measurement of MV-TF activity more compatible with clinical practice and open the way
 521 for future automation.

522

523 Tables

	All MV	PMV	EryMV	GranMV	HLADR MV	
HS-C	82±10	91±9	43±16	87±5	82±10	
Ctrl IMS	3±3	5±7	0	2±7	3±2	
Lineage specific antigens	CD41 IMS	50±13	98±3	19±16	33±36	23±27.2
	CD15 IMS	22±11	18±16	0	92±4	22±20
	HLA-DR IMS	27±6	13±11	0	19±14	84±15
Widely represented antigens	CD29 IMS	58±17	93±3	11±17	41±22	78±10
	CD55 IMS	49±16	63±21	55±26	52±20	59±20
	CD59 IMS	48±28	52±33	66±45	70±25	47±20

	HLA-ABC IMS	66±13	83±9	23±23	75±10	75±17
	CD29-59 IMS	84±7	97±3	83±10	91±1	89±4

524

525 **Table 1. Efficacy of MV depletion as measured by high sensitivity flow cytometry.**

526 Three platelet-free plasma (PFP) samples from three patients were treated with i) a high-speed
527 centrifugation (HS-C) or ii) an IMS-based isolation protocol (different specificities were
528 used). The results indicate the percentage of microvesicle (MV) depletion in each sub-
529 population compared to the original sample (reference for 0% depletion). Grey shading
530 indicates that MV depletion is better than or equal to HS-C. The various gates of interest in
531 the flow cytometry protocol were defined via labeling with Annexin V-FITC (“All MV”),
532 CD41-PE (PMV), CD235a-AF750 (EryMV), CD15-BV650 (GranMV), and anti-HLA-DR-
533 PE (Mono and B-lymphocyte-MV). HS-C: high-speed centrifugation; Ctrl IMS: A non-
534 reactive antibody was coated on the IMS beads.

	Sample	MV-TF level	MV isolation	Number of samples	Number of operators	CV (%)
Repeatability 1	BxPC-3 PFP	High	HS-C	3	1	37
			CD29-59 IMS	3	1	1.2
Repeatability 2	LPS-act. PFP	Medium	HS-C	3	1	20
			CD29-59 IMS	3	1	8.1
Repeatability 3	Unstim. PFP	Low	HS-C	3	1	19
			CD29-59 IMS	3	1	17
Inter-operator reproducibility 1	BxPC-3 PFP	High	HS-C	3	3	35
			CD29-59 IMS	3	3	10
Inter-operator reproducibility 2	LPS-act. PFP	Medium	HS-C	3	3	16
			CD29-59 IMS	3	3	7
Inter-operator reproducibility 3	Unstim. PFP	Low	HS-C	3	3	33
			CD29-59 IMS	3	3	18

535

536 **Table 2. Comparison of reproducibility between optimized IMS- and HS-C-based MV-**
537 **TF assays.** BxPC-3 PFP: MV BxPC-3 spiked into PFP, unstimulated PFP (Unstim PFP) and
538 LPS-activated plasma (LPS-act. PFP). HS-C: high-speed centrifugation; IMS:
539 immunomagnetic separation.

540

541 Figure legends

542 **Figure 1: IMS-based MV isolation depends on the beads' specificity.** A. Flow cytometry-
543 based quantitation of residual MV before and after depletion with IMS (Immunomagnetic
544 separation) or centrifugation. All results were obtained on CytoFLEX®, and actual events
545 were previously gated on VSSC-H (violet side scatter height) using a Gigamix-Plus strategy.
546 The various gates of interest were defined by labelling with Annexin V-FITC (All MV),
547 CD15-BV650 (GranMV), CD41-PE (PMV), and HLA-DR-PE (Mono and B lymphocyte -
548 MV). In a representative experiment, the last column shows the absolute number of MV
549 remaining after isolation in supernatants (SN) in the same sample volume, i.e. MV not
550 collected by [CD55 IMS beads \(among all AnnV+ MV\)](#), CD15 IMS beads (among CD15+
551 MV), CD41 IMS beads (among CD41 MV), and anti-HLA-DR IMS beads (among HLA-DR+
552 MV). B. The depletion efficiency for each MV subset is compared between high-speed
553 centrifugation (HS-C) and CD29-59 IMS (mean+/-s.d. values from three different platelet-
554 free plasma). NS: $p > 0.05$; *: $p < 0.05$.

555 **Figure 2: Comparison of CD29-59 IMS-based and high-speed centrifugation-**
556 **based MV-TF activity assays in different body fluids and the impact of**
557 **TFPI**

558 **A.** Comparison of yields between centrifugation (HS-C, 100%) and CD29-59 IMS in saliva
559 (n=6), pleural fluids (n=4), HEPES buffer, or plasma samples spiked with purified cancer
560 MV-TF (n=4). **B.** Inhibition of MV-TF activity by non-specific adsorption of TFPI on IMS
561 beads. A wide range of TFPI concentrations (0-1500 ng) in HEPES buffer was added on a-
562 DNP Mab-coated (sham-) IMS beads. After 60 minutes, sham-IMS beads were washed and
563 incubated with BxPC-3 MV before measuring the MV-TF activity. The physiological
564 plasmatic concentrations of TFPI are indicated in the graph as “TFPI normal values” **C.**
565 Efficacy of anti TFPI (α -TFPI) to neutralize the inhibitory effect of TFPI on MV-TF activity.
566 MV-TF activity was measured on BxPC3 MV in the absence or presence of sham-IMS beads
567 (μ S) previously incubated with normal plasma (NP), TFPI-immunodepleted plasma (DEF), or
568 NP with anti-TFPI antibody. Each sample (n) was treated in triplicate. NS: $p>0.05$; *:
569 $p<0.05$; **: $p<0.01$; and ***: $p<0.001$.

570 **Figure 3: Optimization of experimental conditions in the bead-based MV-TF activity**
571 **assay.** The amount of beads and incubation time were key factors to optimize when
572 outperforming the centrifugation-based isolation method **A.** N to 4N amounts of CD29-59
573 IMS beads (white bars) were compared to high-speed centrifugation (Grey bar, HS-C, 100%)
574 on 100 μ l of PFP from LPS-activated blood. The activity levels after IMS isolation were
575 compared to those gained via centrifugation. **B.** 3N (white bars) and 6N (dark grey bars) show
576 the amount of CD29-59 IMS beads tested at 15, 30, 45, and 60 min and compared to high-
577 speed centrifugation (grey bar, HS-C, 100%) (2 x 60 min 24000 g) (mean values from
578 triplicates). NS: $p>0.05$; *: $p<0.05$; **: $p<0.01$; and ***: $p<0.001$.

579 **Figure 4: Comparison of analytical performance between optimized IMS- and HS-C-**
580 **based MV-TF assays.** A and B. Sensitivity. MV-TF activity was measured on BxPC-3 MV
581 spiked into PFP (A) (n=9 i.e. 3x3 performed by 3 different operators) or (B) on 11 PFP w/o

582 LPS stimulation. C. Specificity. MV-TF activity was measured on HAP1- (grey bars) and
583 KO-TF-HAP1- (white bars) MV spiked in PFP. Ctrl IMS: IMS beads coated with an
584 irrelevant antibody (anti-DNP). The dotted line represents the limit of quantification. (n=3) D.
585 Linearity. MV-TF activity was measured on HAP1-MV spiked in PFP at various levels (n=3).
586 HS-C: high-speed centrifugation; IMS: immunomagnetic separation. **: p<0.01 and ***:
587 p<0.001.

588 **Figure 5: Selection of an effective panel of monoclonal antibodies to identify the pro-**
589 **coagulant subpopulations of MV in the LPS model and an example of cancer pleural**
590 **fluid** (A) Results of multiple IMS isolations of MV-TF activity (vs. centrifugation as a
591 reference). CD29-59 reference IMS (Grey bar). (B) Immunocapture of different MV subsets
592 compared to CD29-59 IMS in the LPS model. (C) Immunocapture of different MV subsets
593 compared to CD29-59 IMS in a sample of cancer pleural fluid (values from triplicates).

594 Funding sources

595

596 C.F. was supported by ANRT (Association Nationale de la Recherche et de la Technologie) in
597 the context of the CIFRE system.

598 Declaration of Competing Interest

599

600 We disclose as a conflict of interest that P. P, T. B, and C. J are full-time employees of
601 Biocytex. F. DG and R.L disclose grants from Stago and a patent on microvesicle fibrinolytic
602 activity licensed to Stago.

603 Citations

604

- 605 1.R. Lacroix, L. Vallier, A. Bonifay, S. Simoncini, D. Mege, M. Aubert, L. Panicot-Dubois, C.
606 Dubois and F. Dignat-George, Microvesicles and Cancer Associated Thrombosis,
607 *Semin. Thromb. Hemost.* **45** (2019) 593–603.; DOI:10.1055/s-0039-1693476
- 608 2.A.-L. Ståhl, K. Johansson, M. Mossberg, R. Kahn and D. Karpman, Exosomes and
609 microvesicles in normal physiology, pathophysiology, and renal diseases, *Pediatr.*
610 *Nephrol. Berl. Ger.* **34** (2019) 11–30.; DOI:10.1007/s00467-017-3816-z
- 611 3.S. Nomura, M. Niki, T. Nisizawa, T. Tamaki and M. Shimizu, Microparticles as Biomarkers
612 of Blood Coagulation in Cancer, *Biomark. Cancer* **7** (2015) 51–56.;
613 DOI:10.4137/BIC.S30347
- 614 4.Y. Chen, G. Li and M.-L. Liu, Microvesicles as Emerging Biomarkers and Therapeutic
615 Targets in Cardiometabolic Diseases, *Genomics Proteomics Bioinformatics* **16** (2018)
616 50–62.; DOI:10.1016/j.gpb.2017.03.006
- 617 5.A. P. Owens 3rd and N. Mackman, Microparticles in hemostasis and thrombosis, *Circ. Res.*
618 **108** (2011) 1284–1297.; DOI:10.1161/CIRCRESAHA.110.233056
- 619 6.R. F. A. Zwaal and A. J. Schroit, Pathophysiologic Implications of Membrane Phospholipid
620 Asymmetry in Blood Cells, *Blood* **89** (1997) 1121.; DOI:PMID: 9516159
- 621 7.N. Satta, F. Toti, O. Feugeas, A. Bohbot, J. Dachary-Prigent, V. Eschwège, H. Hedman and
622 J. M. Freyssinet, Monocyte vesiculation is a possible mechanism for dissemination of
623 membrane-associated procoagulant activities and adhesion molecules after stimulation
624 by lipopolysaccharide, *J. Immunol. Baltim. Md 1950* **153** (1994) 3245–3255.;
625 DOI:PMID: 7522256
- 626 8.S. Butenas, B. A. Bouchard, K. E. Brummel-Ziedins, B. Parhami-Seren and K. G. Mann,
627 Tissue factor activity in whole blood, *Blood* **105** (2005) 2764.; DOI:10.1182/blood-
628 2004-09-3567

- 629 9.J. L. Yu, L. May, V. Lhotak, S. Shahrzad, S. Shirasawa, J. I. Weitz, B. L. Coomber, N.
630 Mackman and J. W. Rak, Oncogenic events regulate tissue factor expression in
631 colorectal cancer cells: implications for tumor progression and angiogenesis, *Blood*
632 **105** (2005) 1734–1741.; DOI:10.1182/blood-2004-05-2042
- 633 10.M. Davila, A. Amirkhosravi, E. Coll, R. D. Liza and J. Francis, Tissue Factor-Bearing
634 Microparticles Derived from Tumor Cells: Impact on Coagulation Activation., *Blood*
635 **108** (2006) 1757–1757.; DOI:10.1182/blood.V108.11.1757.1757
- 636 11.S. Falati, Q. Liu, P. Gross, G. Merrill-Skoloff, J. Chou, E. Vandendries, A. Celi, K. Croce,
637 B. C. Furie and B. Furie, Accumulation of tissue factor into developing thrombi in
638 vivo is dependent upon microparticle P-selectin glycoprotein ligand 1 and platelet P-
639 selectin, *J. Exp. Med.* **197** (2003) 1585–1598.; DOI:10.1084/jem.20021868
- 640 12.E. Ramacciotti, A. E. Hawley, D. M. Farris, N. E. Ballard, S. K. Wroblewski, D. D. Myers Jr,
641 P. K. Henke and T. W. Wakefield, Leukocyte- and platelet-derived microparticles
642 correlate with thrombus weight and tissue factor activity in an experimental mouse
643 model of venous thrombosis, *Thromb. Haemost.* **101** (2009) 748–754.; DOI:PMID:
644 19350121
- 645 13.F. J. S. H. Woei-A-Jin, M. E. T. Tesselaar, P. Garcia Rodriguez, F. P. H. T. M. Romijn, R.
646 M. Bertina and S. Osanto, Tissue factor-bearing microparticles and CA19.9: two
647 players in pancreatic cancer-associated thrombosis?, *Br. J. Cancer* **115** (2016) 332–
648 338.; DOI:10.1038/bjc.2016.170
- 649 14.A. Bharthuar, A. A. Khorana, A. Hutson, J.-G. Wang, N. S. Key, N. Mackman and R. V.
650 Iyer, Circulating microparticle tissue factor, thromboembolism and survival in
651 pancreaticobiliary cancers, *Thromb. Res.* **132** (2013) 180–184.;
652 DOI:10.1016/j.thromres.2013.06.026

- 653 15.M. T. Sartori, A. Della Puppa, A. Ballin, E. Campello, C. M. Radu, G. Saggiorato, D.
654 d'Avella, R. Scienza, G. Cella and P. Simioni, Circulating microparticles of glial
655 origin and tissue factor bearing in high-grade glioma: a potential prothrombotic role,
656 *Thromb. Haemost.* **110** (2013) 378–385.; DOI:10.1160/TH12-12-0957
- 657 16.D. Faille, M.-C. Bourrienne, E. de Raucourt, L. de Chaisemartin, V. Granger, R. Lacroix,
658 L. Panicot-Dubois, P. Hammel, P. Lévy, P. Ruszniewski, N. Ajzenberg and V.
659 Rebours, Biomarkers for the risk of thrombosis in pancreatic adenocarcinoma are
660 related to cancer process, *Oncotarget* **9** (2018) 26453–26465.;
661 DOI:10.18632/oncotarget.25458
- 662 17.Y. Hisada and N. Mackman, Cancer-associated pathways and biomarkers of venous
663 thrombosis, *Blood* **130** (2017) 1499–1506.; DOI:10.1182/blood-2017-03-743211
- 664 18.Y. Hisada and N. Mackman, Measurement of tissue factor activity in extracellular vesicles
665 from human plasma samples, *Res. Pract. Thromb. Haemost.* **3** (2018) 44–48.;
666 DOI:10.1002/rth2.12165
- 667 19.S. P. Grover and N. Mackman, Tissue Factor: An Essential Mediator of Hemostasis and
668 Trigger of Thrombosis, *Arterioscler. Thromb. Vasc. Biol.* **38** (2018) 709–725.;
669 DOI:10.1161/ATVBAHA.117.309846
- 670 20.R. D. Lee, D. A. Barcel, J. C. Williams, J. G. Wang, J. C. Boles, D. A. Manly, N. S. Key
671 and N. Mackman, Pre-analytical and analytical variables affecting the measurement of
672 plasma-derived microparticle tissue factor activity, *Thromb. Res.* **129** (2012) 80–85.;
673 DOI:10.1016/j.thromres.2011.06.004
- 674 21.H. C. Hemker, P. Giesen, R. AlDieri, V. Regnault, E. de Smed, R. Wagenvoort, T.
675 Lecompte and S. Béguin, The Calibrated Automated Thrombogram (CAT): a
676 universal routine test for hyper- and hypocoagulability, *Pathophysiol. Haemost.*
677 *Thromb.* **32** (2002) 249–253.; DOI:10.1159/000073575

678 22.T. Exner, J. Joseph, J. Low, D. Connor and D. Ma, A new activated factor X-based clotting
679 method with improved specificity for procoagulant phospholipid, *Blood Coagul.*
680 *Fibrinolysis Int. J. Haemost. Thromb.* **14** (2003) 773–779.; DOI:10.1097/00001721-
681 200312000-00015

682 23.R. J. Berckmans, A. Sturk, L. M. van Tienen, M. C. L. Schaap and R. Nieuwland, Cell-
683 derived vesicles exposing coagulant tissue factor in saliva, *Blood* **117** (2011) 3172.;
684 DOI:10.1182/blood-2010-06-290460

685 24.L. Vallier, T. Bouriche, A. Bonifay, C. Judicone, J. Bez, C. Franco, C. Guervilly, Y.
686 Hisada, N. Mackman, R. Houston, P. Poncelet, F. Dignat-George and R. Lacroix,
687 Increasing the sensitivity of the human microvesicle tissue factor activity assay,
688 *Thromb. Res.* **182** (2019) 64–74.; DOI:10.1016/j.thromres.2019.07.011

689 25.R. Linares, S. Tan, C. Gounou, N. Arraud and A. R. Brisson, High-speed centrifugation
690 induces aggregation of extracellular vesicles, *J. Extracell. Vesicles* **4** (2015) 29509–
691 29509.; DOI:10.3402/jev.v4.29509

692 26.Å. Thulin, C. Christersson, J. Alfredsson and A. Siegbahn, Circulating cell-derived
693 microparticles as biomarkers in cardiovascular disease, *Biomark. Med.* **10** (2016)
694 1009–1022.; DOI:10.2217/bmm-2016-0035

695 27.C. Théry, K. W. Witwer, E. Aikawa, M. J. Alcaraz, J. D. Anderson, R. Andriantsitohaina,
696 A. Antoniou, T. Arab, F. Archer, G. K. Atkin-Smith, D. C. Ayre, J.-M. Bach, D.
697 Bachurski, H. Baharvand, L. Balaj, S. Baldacchino, N. N. Bauer, A. A. Baxter, et al.,
698 Minimal information for studies of extracellular vesicles 2018 (MISEV2018): a
699 position statement of the International Society for Extracellular Vesicles and update of
700 the MISEV2014 guidelines, *J. Extracell. Vesicles* **7** (2018) 1535750–1535750.;
701 DOI:10.1080/20013078.2018.1535750

- 702 28.E. Roca, R. Lacroix, C. Judicone, S. Laroumagne, S. Robert, S. Cointe, A. Muller, E.
703 Kaspi, P. Roll, A. R. Brisson, C. Tantucci, P. Astoul and F. Dignat-George, Detection
704 of EpCAM-positive microparticles in pleural fluid: A new approach to mini-invasively
705 identify patients with malignant pleural effusions, *Oncotarget* **7** (2015) 3357–3366.;
706 DOI:10.18632/oncotarget.6581
- 707 29.P. Poncelet, S. Robert, T. Bouriche, J. Bez, R. Lacroix and F. Dignat-George, Standardized
708 counting of circulating platelet microparticles using currently available flow
709 cytometers and scatter-based triggering: Forward or side scatter?, *Cytometry A* **89**
710 (2016) 148–158.; DOI:10.1002/cyto.a.22685
- 711 30.S. Cointe, C. Judicone, S. Robert, M. J. Mooberry, P. Poncelet, M. Wauben, R. Nieuwland,
712 N. S. Key, F. Dignat-George and R. Lacroix, Standardization of microparticle
713 enumeration across different flow cytometry platforms: results of a multicenter
714 collaborative workshop, *J. Thromb. Haemost. JTH* **15** (2017) 187–193.;
715 DOI:10.1111/jth.13514
- 716 31.N. S. Key, A. Slungaard, L. Dandele, S. C. Nelson, C. Moertel, L. A. Styles, F. A.
717 Kuypers and R. R. Bach, Whole Blood Tissue Factor Procoagulant Activity Is
718 Elevated in Patients With Sickle Cell Disease, *Blood* **91** (1998) 4216–4223.;
719 DOI:10.1182/blood.V91.11.4216
- 720 32.É. Biró, K. N. Sturk-Maquelin, G. M. T. Vogel, D. G. Meuleman, M. J. Smit, C. E. Hack,
721 A. Sturk and R. Nieuwland, Human cell-derived microparticles promote thrombus
722 formation in vivo in a tissue factor-dependent manner, *J. Thromb. Haemost.* **1** (2003)
723 2561–2568.; DOI:10.1046/j.1538-7836.2003.00456.x
- 724 33.F. Siddiqui, A. Tafur, L. S. Ramacciotti, W. Jeske, D. Hoppensteadt, E. Ramacciotti, O.
725 Iqbal and J. Fareed, Reversal of Factor Xa Inhibitors by Andexanet Alfa May Increase
726 Thrombogenesis Compared to Pretreatment Values, *Clin. Appl. Thromb. Off. J. Int.*

727 *Acad. Clin. Appl. Thromb.* **25** (2019) 1076029619863493–1076029619863493.;

728 DOI:10.1177/1076029619863493

729 34.O. Aras, A. Shet, R. R. Bach, J. L. Hysjulien, A. Slungaard, R. P. Hebbel, G. Escolar, B.

730 Jilma and N. S. Key, Induction of microparticle- and cell-associated intravascular

731 tissue factor in human endotoxemia, *Blood* **103** (2004) 4545–4553.;

732 DOI:10.1182/blood-2003-03-0713

733 35.M. Y. Konoshenko, E. A. Lekchnov, A. V. Vlassov and P. P. Laktionov, Isolation of

734 Extracellular Vesicles: General Methodologies and Latest Trends, *BioMed Res. Int.*

735 **2018** (2018) 8545347–8545347.; DOI:10.1155/2018/8545347

736 36.L. M. Doyle and M. Z. Wang, Overview of Extracellular Vesicles, Their Origin,

737 Composition, Purpose, and Methods for Exosome Isolation and Analysis, *Cells* **8**

738 (2019) 727.; DOI:10.3390/cells8070727

739 37.J. Van Deun, P. Mestdagh, R. Sormunen, V. Cocquyt, K. Vermaelen, J. Vandesompele, M.

740 Bracke, O. De Wever and A. Hendrix, The impact of disparate isolation methods for

741 extracellular vesicles on downstream RNA profiling, *J. Extracell. Vesicles* **3** (2014)

742 10.3402/jev.v3.24858.; DOI:10.3402/jev.v3.24858

743 38.R. J. Lobb, M. Becker, S. W. Wen, C. S. F. Wong, A. P. Wiegmans, A. Leimgruber and A.

744 Möller, Optimized exosome isolation protocol for cell culture supernatant and human

745 plasma, *J. Extracell. Vesicles* **4** (2015) 27031–27031.; DOI:10.3402/jev.v4.27031

746 39.A. Gámez-Valero, M. Monguió-Tortajada, L. Carreras-Planella, M. la Franquesa, K. Beyer

747 and F. E. Borràs, Size-Exclusion Chromatography-based isolation minimally alters

748 Extracellular Vesicles' characteristics compared to precipitating agents, *Sci. Rep.* **6**

749 (2016) 33641–33641.; DOI:10.1038/srep33641

750 40.A. N. Böing, E. van der Pol, A. E. Grootemaat, F. A. W. Coumans, A. Sturk and R.

751 Nieuwland, Single-step isolation of extracellular vesicles by size-exclusion

752 chromatography, *J. Extracell. Vesicles* **3** (2014) 10.3402/jev.v3.23430.;

753 DOI:10.3402/jev.v3.23430

754 41.F. Momen-Heravi, L. Balaj, S. Alian, P.-Y. Mantel, A. E. Halleck, A. J. Trachtenberg, C.

755 E. Soria, S. Oquin, C. M. Bonebreak, E. Saracoglu, J. Skog and W. P. Kuo, Current

756 methods for the isolation of extracellular vesicles, *Biol. Chem.* **394** (2013) 1253–1262.;

757 DOI:10.1515/hsz-2013-0141

758 42.J. Webber and A. Clayton, How pure are your vesicles?, *J. Extracell. Vesicles* **2** (2013)

759 10.3402/jev.v2i0.19861.; DOI:10.3402/jev.v2i0.19861

760 43.T. Baranyai, K. Herczeg, Z. Onódi, I. Voszka, K. Módos, N. Marton, G. Nagy, I. Mäger,

761 M. J. Wood, S. El Andaloussi, Z. Pálincás, V. Kumar, P. Nagy, Á. Kittel, E. I. Buzás,

762 P. Ferdinandy and Z. Giricz, Isolation of Exosomes from Blood Plasma: Qualitative

763 and Quantitative Comparison of Ultracentrifugation and Size Exclusion

764 Chromatography Methods, *PLoS One* **10** (2015) e0145686–e0145686.;

765 DOI:10.1371/journal.pone.0145686

766 44.A. Morales-Kastresana, T. A. Musich, J. A. Welsh, W. Telford, T. Demberg, J. C. S. Wood,

767 M. Bigos, C. D. Ross, A. Kachynski, A. Dean, E. J. Felton, J. Van Dyke, J. Tigges, V.

768 Toxavidis, D. R. Parks, W. R. Overton, A. H. Kesarwala, G. J. Freeman, et al., High-

769 fidelity detection and sorting of nanoscale vesicles in viral disease and cancer, *J.*

770 *Extracell. Vesicles* **8** (2019) 1597603.; DOI:10.1080/20013078.2019.1597603

771 45.A. Liga, A. D. B. Vliegthart, W. Oosthuyzen, J. W. Dear and M. Kersaudy-Kerhoas,

772 Exosome isolation: a microfluidic road-map, *Lab. Chip* **15** (2015) 2388–2394.;

773 DOI:10.1039/C5LC00240K

774 46.C. Chen, B.-R. Lin, M.-Y. Hsu and C.-M. Cheng, Paper-based devices for isolation and

775 characterization of extracellular vesicles, *J. Vis. Exp. JoVE* (2015) e52722–e52722.;

776 DOI:10.3791/52722

- 777 47.Å. Thulin, J. Yan, M. Åberg, C. Christersson, M. Kamali-Moghaddam and A. Siegbahn,
778 Sensitive and Specific Detection of Platelet-Derived and Tissue Factor-Positive
779 Extracellular Vesicles in Plasma Using Solid-Phase Proximity Ligation Assay, *TH*
780 *Open Companion J. Thromb. Haemost.* **2** (2018) e250–e260.; DOI:10.1055/s-0038-
781 1667204
- 782 48.N. S. Barteneva, E. Fasler-Kan, M. Bernimoulin, J. N. H. Stern, E. D. Ponomarev, L.
783 Duckett and I. A. Vorobjev, Circulating microparticles: square the circle, *BMC Cell*
784 *Biol.* **14** (2013) 23–23.; DOI:10.1186/1471-2121-14-23
- 785 49.D. W. Greening, R. Xu, H. Ji, B. J. Tauro and R. J. Simpson, A protocol for exosome
786 isolation and characterization: evaluation of ultracentrifugation, density-gradient
787 separation, and immunoaffinity capture methods, *Methods Mol. Biol. Clifton NJ* **1295**
788 (2015) 179–209.; DOI:10.1007/978-1-4939-2550-6_15
- 789 50.P. Poncelet, B.-F. I and T. Lavabre-Bertrand, Clinical applications of quantitative
790 immunophenotyping., *Immunophenotyping* (January 2000., pp. 105–132). Wiley-Liss.
- 791 51.G. J. Ruiz-Delgado, E. Vázquez-Garza, N. Méndez-Ramírez and D. Gómez-Almaguer,
792 Abnormalities in the expression of CD55 and CD59 surface molecules on peripheral
793 blood cells are not specific to paroxysmal nocturnal hemoglobinuria, *Hematology* **14**
794 (2009) 33–37.; DOI:10.1179/102453309X385089
- 795 52.H. Rabesandratana, J. P. Toutant, H. Reggio and M. Vidal, Decay-accelerating factor
796 (CD55) and membrane inhibitor of reactive lysis (CD59) are released within exosomes
797 during In vitro maturation of reticulocytes, *Blood* **91** (1998) 2573–2580.; DOI:PMID:
798 9516159
- 799 53.A. de Gassart, C. Géminard, B. Février, G. Raposo and M. Vidal, Lipid raft-associated
800 protein sorting in exosomes, *Blood* **102** (2003) 4336–4344.; DOI:10.1182/blood-2003-
801 03-0871

- 802 54.F. Collino, M. Pomatto, S. Bruno, R. S. Lindoso, M. Tapparo, W. Sicheng, P. Quesenberry
803 and G. Camussi, Exosome and Microvesicle-Enriched Fractions Isolated from
804 Mesenchymal Stem Cells by Gradient Separation Showed Different Molecular
805 Signatures and Functions on Renal Tubular Epithelial Cells, *Stem Cell Rev. Rep.* **13**
806 (2017) 226–243.; DOI:10.1007/s12015-016-9713-1
- 807 55.M. Hellum, I. Franco-Lie, R. Øvstebø, T. Hauge and C. E. Henriksson, The effect of corn
808 trypsin inhibitor, anti-tissue factor pathway inhibitor antibodies and phospholipids on
809 microvesicle-associated thrombin generation in patients with pancreatic cancer and
810 healthy controls, *PLOS ONE* **12** (2017) e0184579.;
811 DOI:10.1371/journal.pone.0184579
- 812 56.K. Tatsumi, S. Antoniak, D. M. Monroe III, A. A. Khorana, N. Mackman and the
813 Subcommittee on Hemostasis and Malignancy, Evaluation of a new commercial assay
814 to measure microparticle tissue factor activity in plasma: communication from the
815 SSC of the ISTH, *J. Thromb. Haemost.* **12** (2014) 1932–1934.;
816 DOI:10.1111/jth.12718
- 817 57.A. Cvjetkovic, J. Lötvall and C. Lässer, The influence of rotor type and centrifugation time
818 on the yield and purity of extracellular vesicles, *J. Extracell. Vesicles* **3** (2014) 23111.;
819 DOI:10.3402/jev.v3.23111
- 820 58.S. Cointe, K. Harti Souab, T. Bouriche, L. Vallier, A. Bonifay, C. Judicone, S. Robert, R.
821 Armand, P. Poncelet, J. Albanese, F. Dignat-George and R. Lacroix, A new assay to
822 evaluate microvesicle plasmin generation capacity: validation in disease with
823 fibrinolysis imbalance, *J. Extracell. Vesicles* **7** (2018) 1494482.;
824 DOI:10.1080/20013078.2018.1494482
- 825 59.K. Meszaros, S. Aberle, R. Dedrick, R. Machovich, A. Horwitz, C. Birr, G. Theofan and J.
826 Parent, Monocyte tissue factor induction by lipopolysaccharide (LPS): dependence on

827 LPS-binding protein and CD14, and inhibition by a recombinant fragment of
828 bactericidal/permeability-increasing protein, *Blood* **83** (1994) 2516.; Retrieved from
829 <http://www.bloodjournal.org/content/83/9/2516.abstract>

830 60.A. N. Barclay, M. H. Brown, S. K. A. Law, A. J. McKnight, M. G. Tomlinson and P. A.
831 van der Merwe, - CD61, In A. N. Barclay, M. H. Brown, S. K. A. Law, A. J.
832 McKnight, M. G. Tomlinson, & P. A. van der Merwe (Eds.), *Leucoc. Antigen*
833 *FactsBook* (pp. 293–294). San Diego: Academic Press.; DOI:10.1016/B978-
834 012078185-0/50500-X

835 61.S. A. Melo, L. B. Luecke, C. Kahlert, A. F. Fernandez, S. T. Gammon, J. Kaye, V. S.
836 LeBleu, E. A. Mittendorf, J. Weitz, N. Rahbari, C. Reissfelder, C. Pilarsky, M. F.
837 Fraga, D. Piwnica-Worms and R. Kalluri, Glypican-1 identifies cancer exosomes and
838 detects early pancreatic cancer, *Nature* **523** (2015) 177–182.;
839 DOI:10.1038/nature14581

840 62.M. Takao, Y. Nagai, M. Ito and T. Ohba, Flow cytometric quantitation of EpCAM-positive
841 extracellular vesicles by immunomagnetic separation and phospholipid staining
842 method, *Genes Cells* **23** (2018) 963–973.; DOI:10.1111/gtc.12645

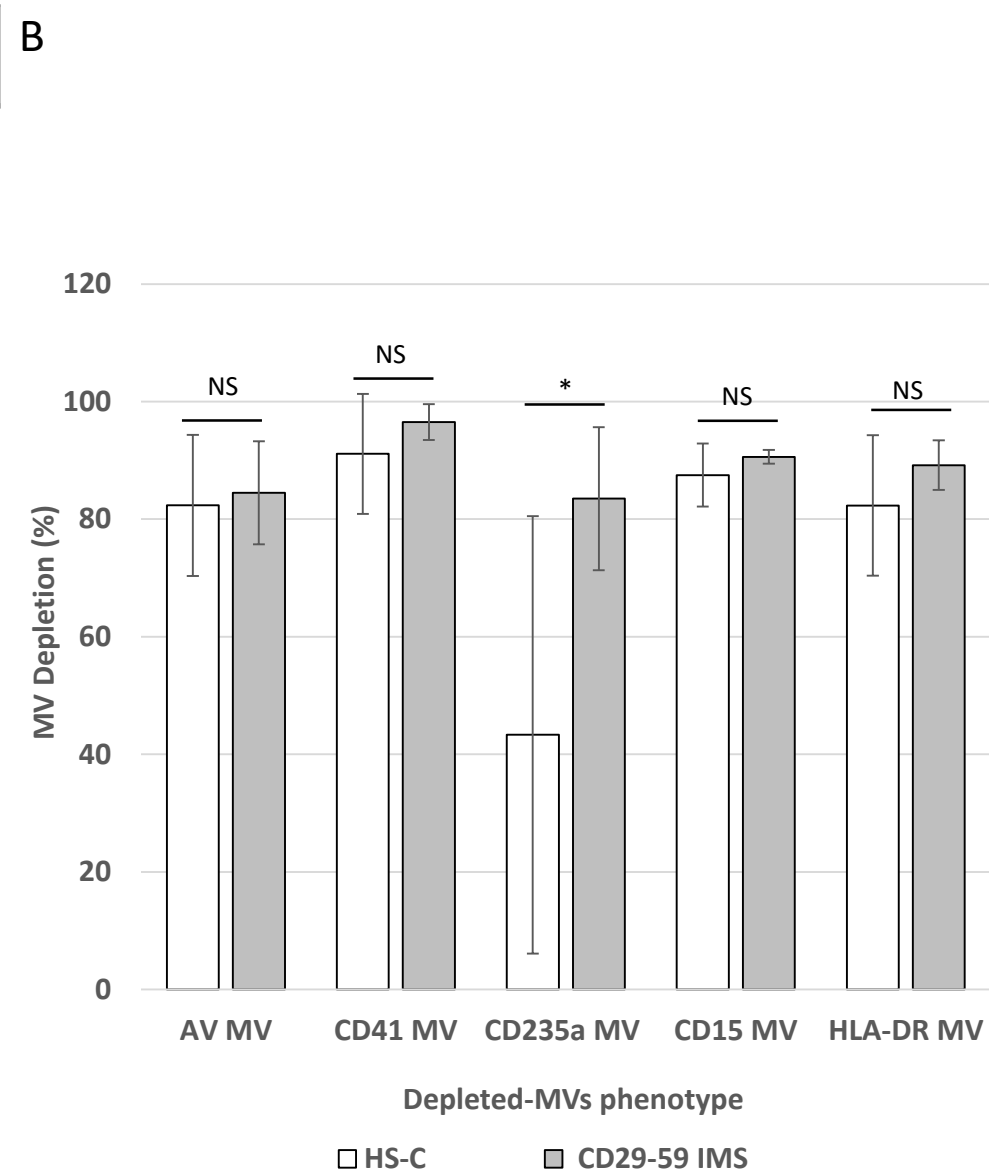
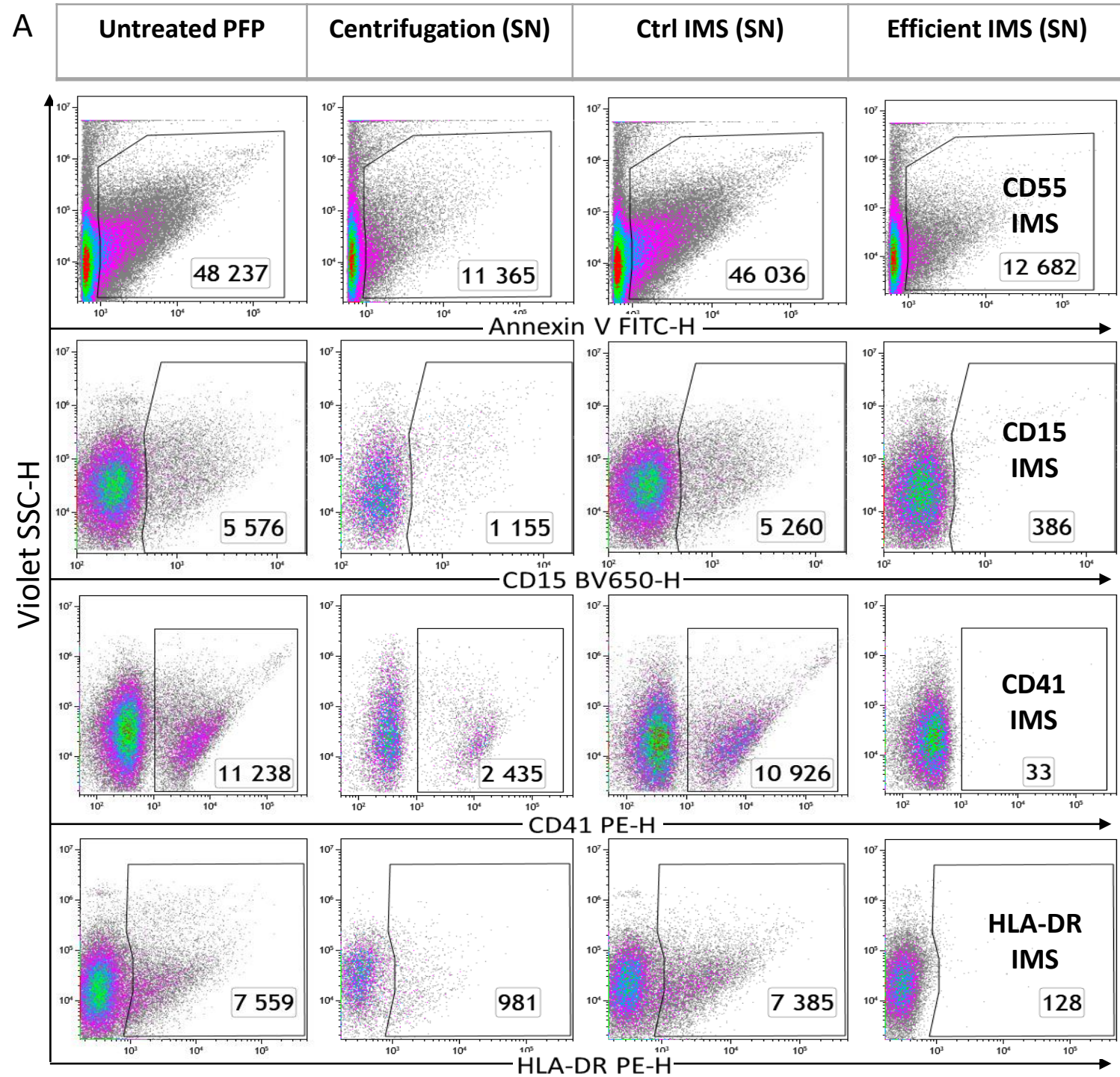
843 63.C. Campos-Silva, H. Suárez, R. Jara-Acevedo, E. Linares-Espinós, L. Martinez-Piñeiro, M.
844 Yáñez-Mó and M. Valés-Gómez, High sensitivity detection of extracellular vesicles
845 immune-captured from urine by conventional flow cytometry, *Sci. Rep.* **9** (2019) 2042.;
846 DOI:10.1038/s41598-019-38516-8

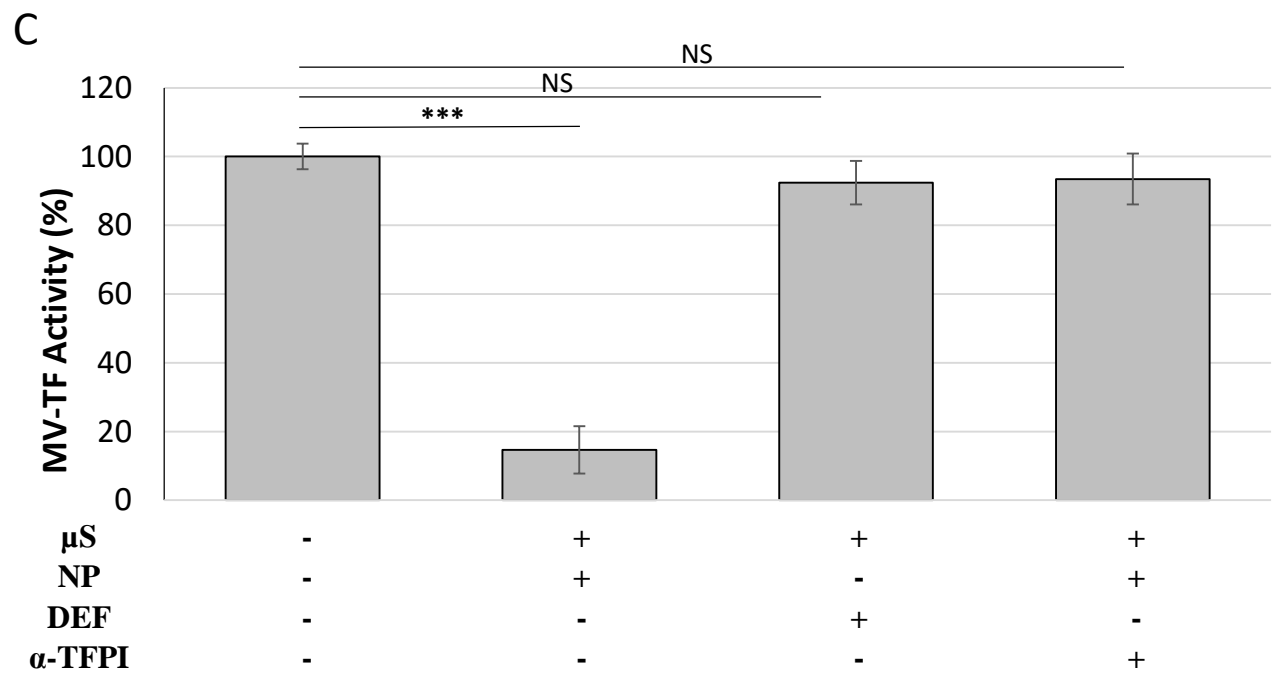
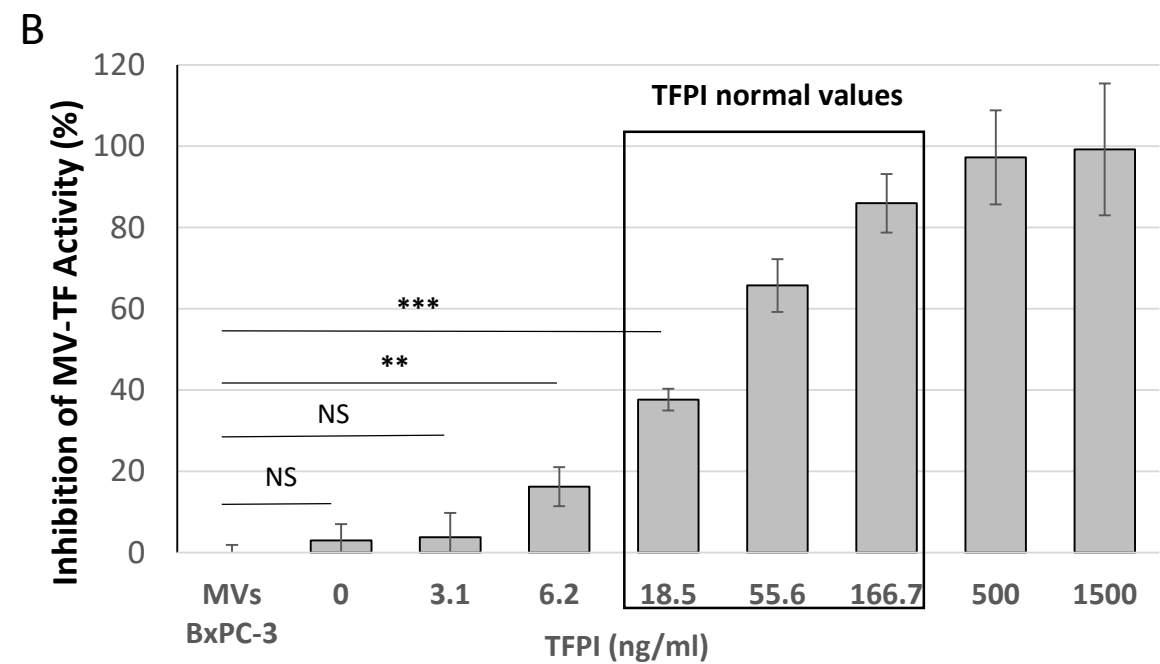
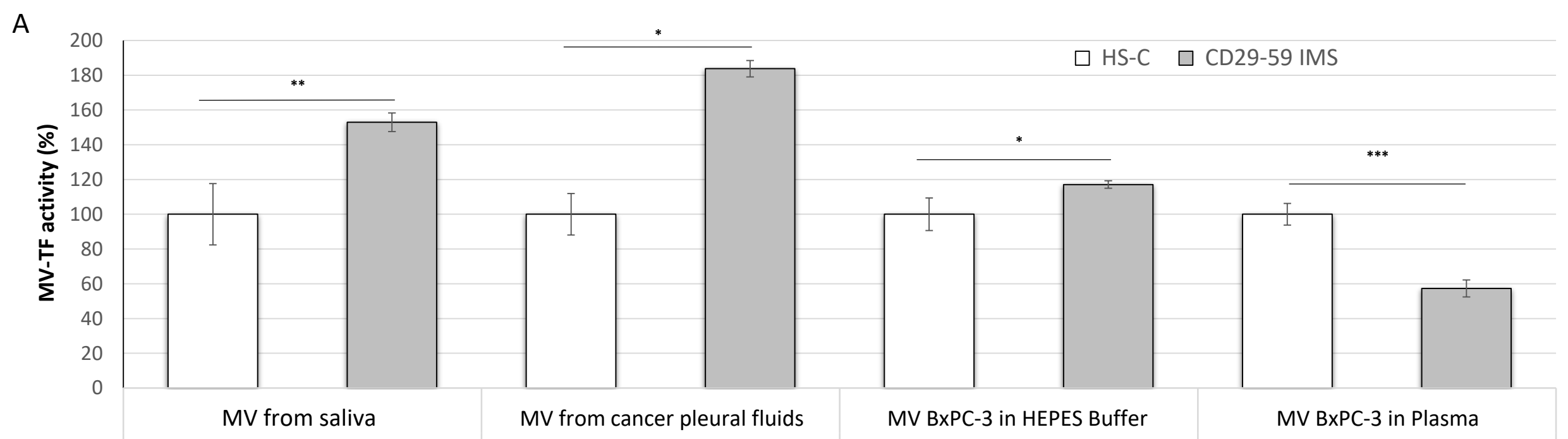
847 64.H. Shao, J. Chung, K. Lee, L. Balaj, C. Min, B. S. Carter, F. H. Hochberg, X. O.
848 Breakefield, H. Lee and R. Weissleder, Chip-based analysis of exosomal mRNA
849 mediating drug resistance in glioblastoma, *Nat. Commun.* **6** (2015) 6999–6999.;
850 DOI:10.1038/ncomms7999

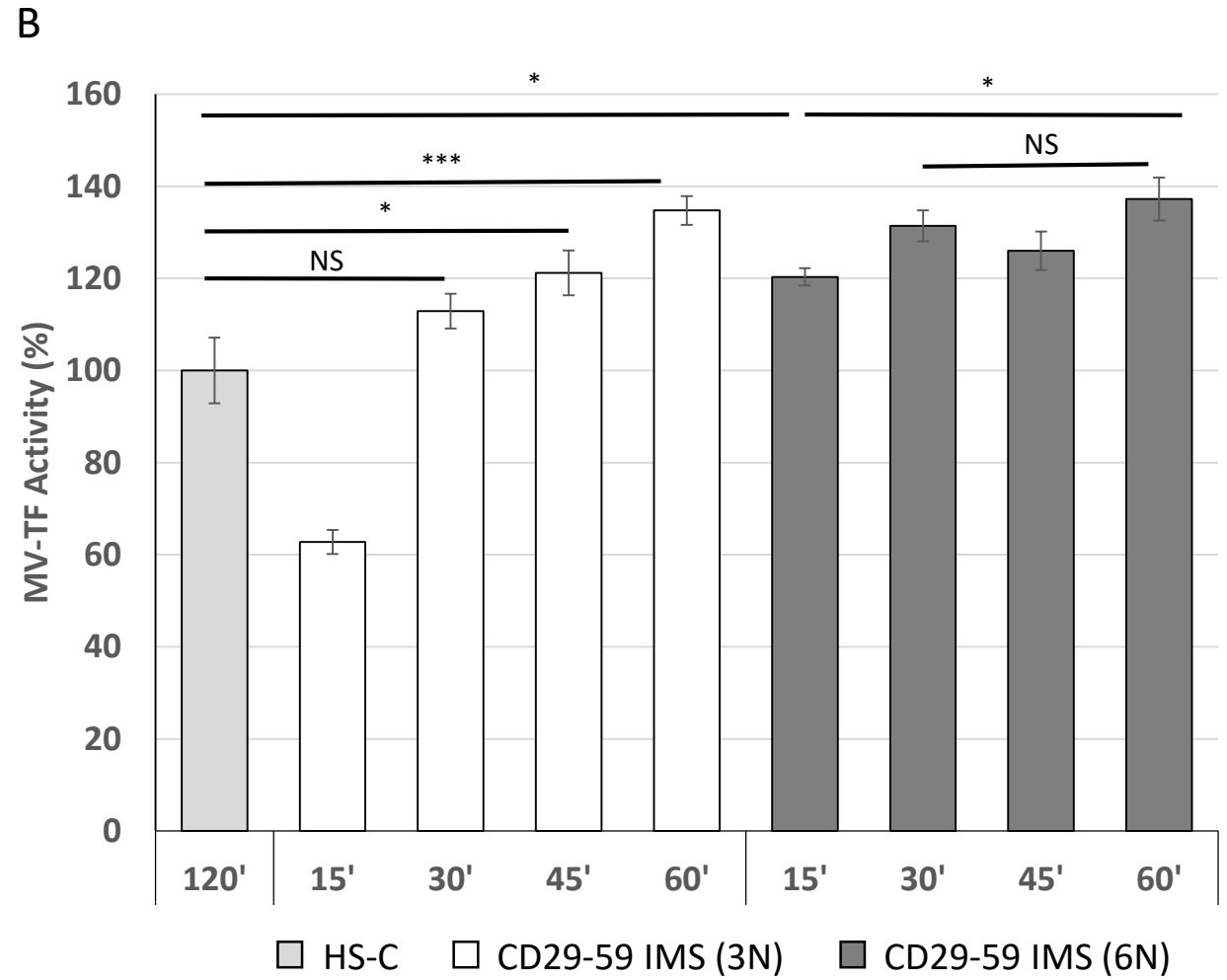
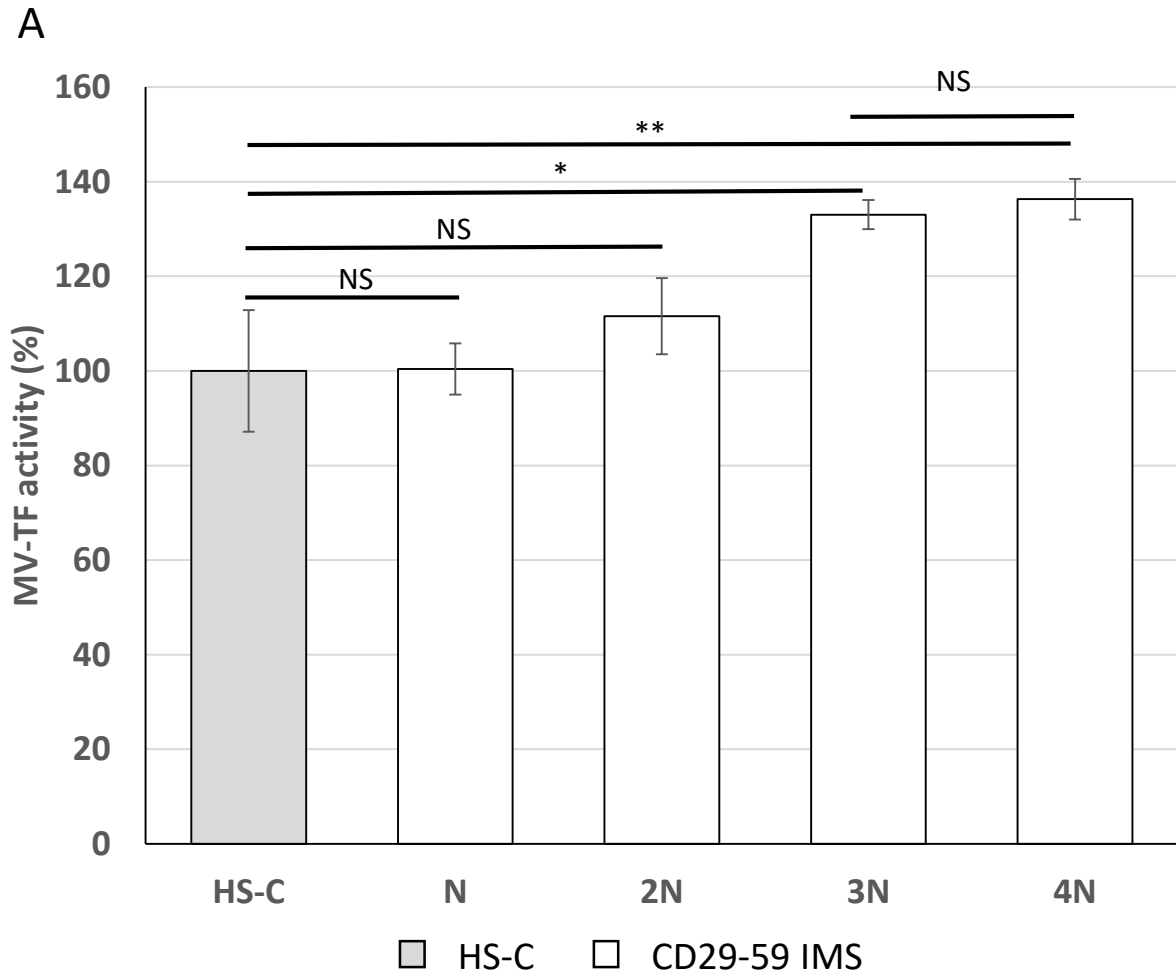
851 65.P. Sharma, S. Ludwig, L. Muller, C. S. Hong, J. M. Kirkwood, S. Ferrone and T. L.
852 Whiteside, Immunoaffinity-based isolation of melanoma cell-derived exosomes from
853 plasma of patients with melanoma, *J. Extracell. Vesicles* **7** (2018) 1435138.;
854 DOI:10.1080/20013078.2018.1435138

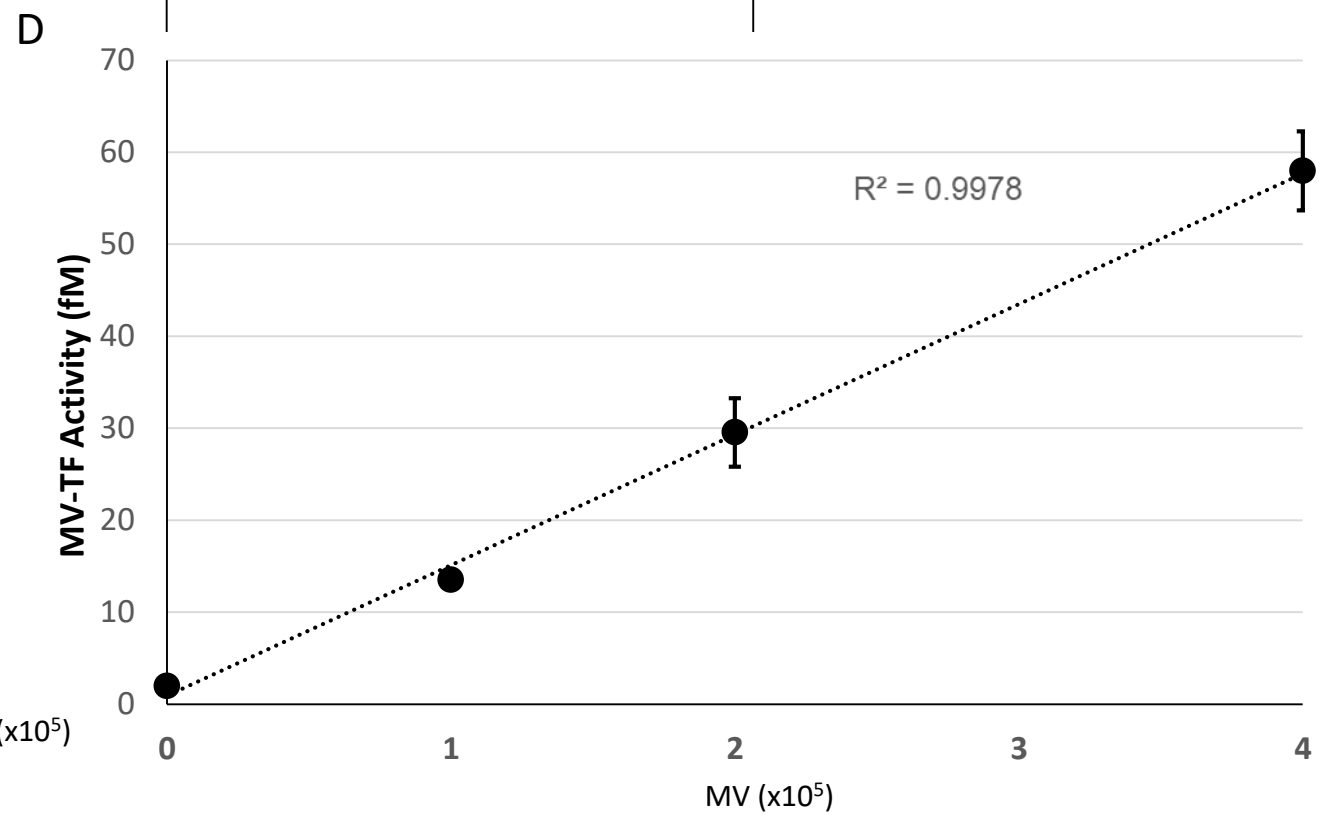
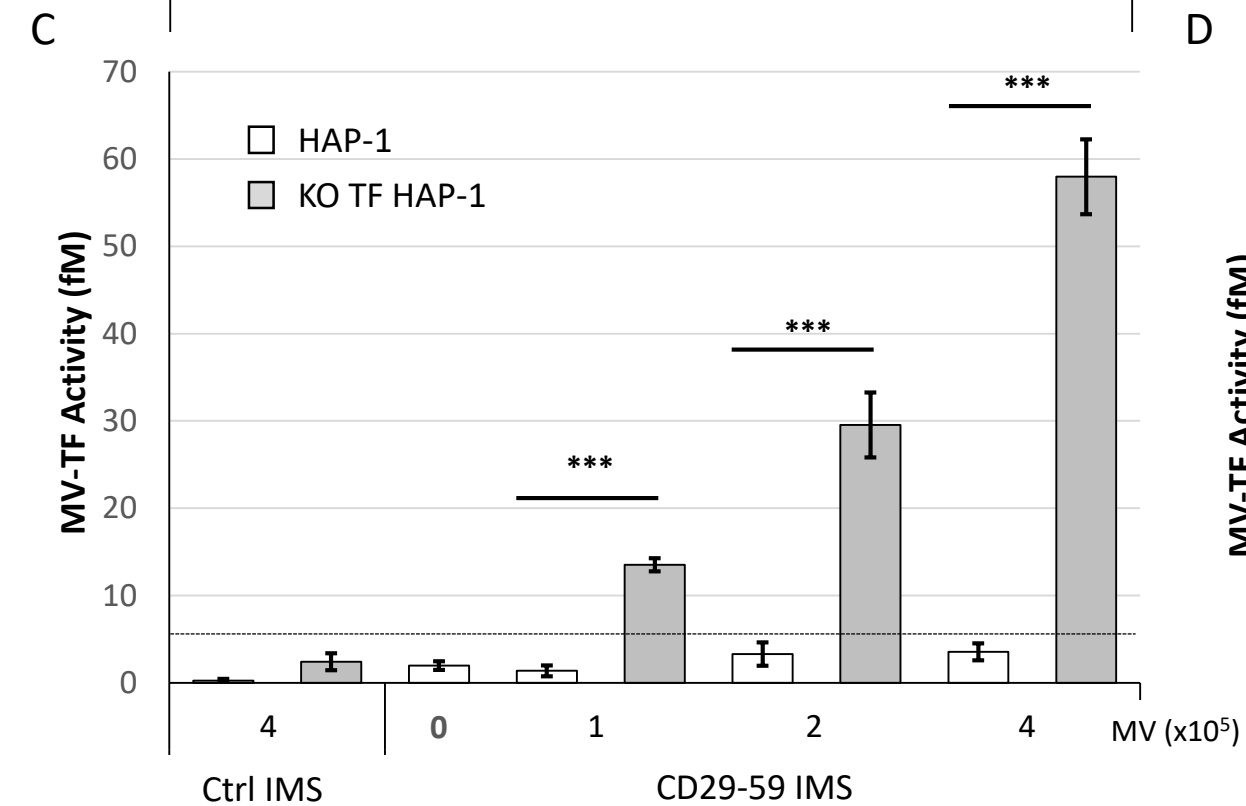
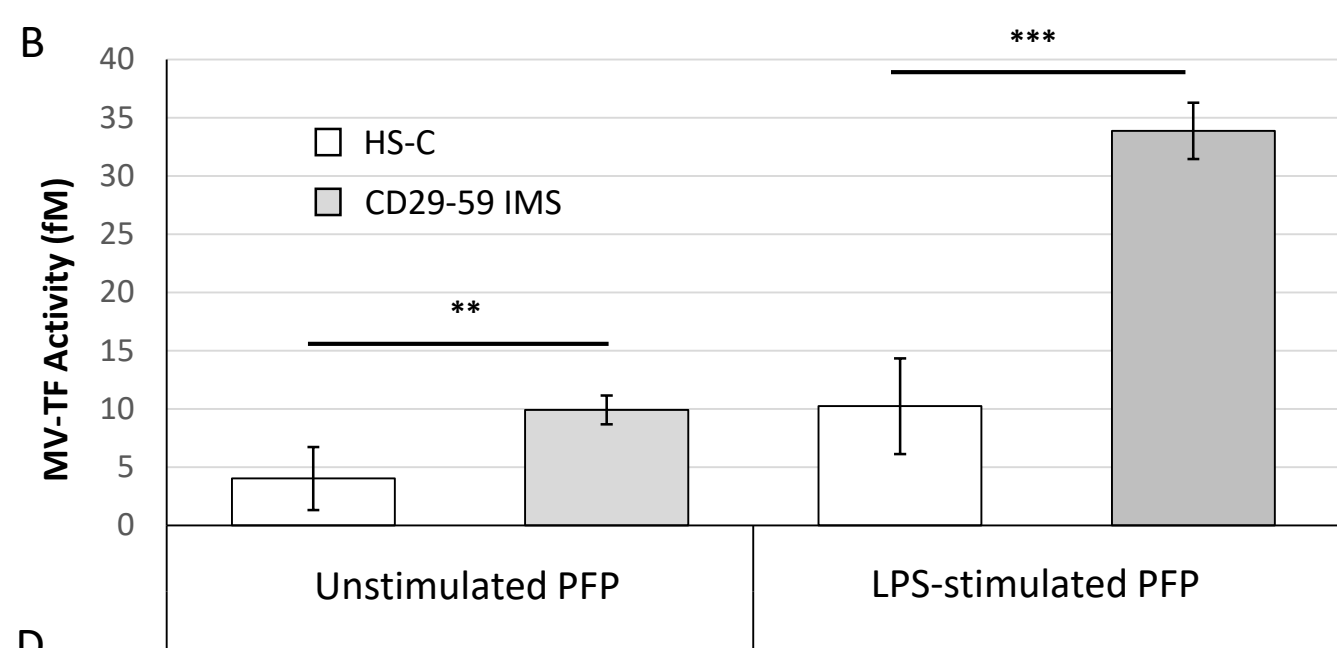
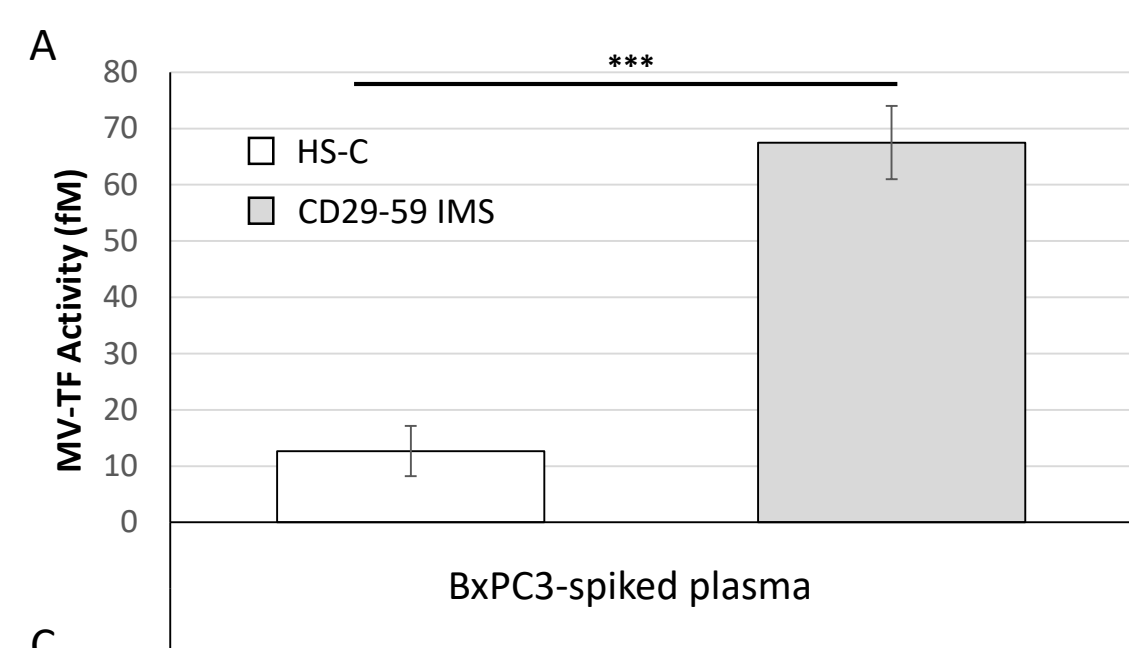
855 66.Z. Zhao, Y. Yang, Y. Zeng and M. He, A microfluidic ExoSearch chip for multiplexed
856 exosome detection towards blood-based ovarian cancer diagnosis, *Lab. Chip* **16** (2016)
857 489–496.; DOI:10.1039/c5lc01117e

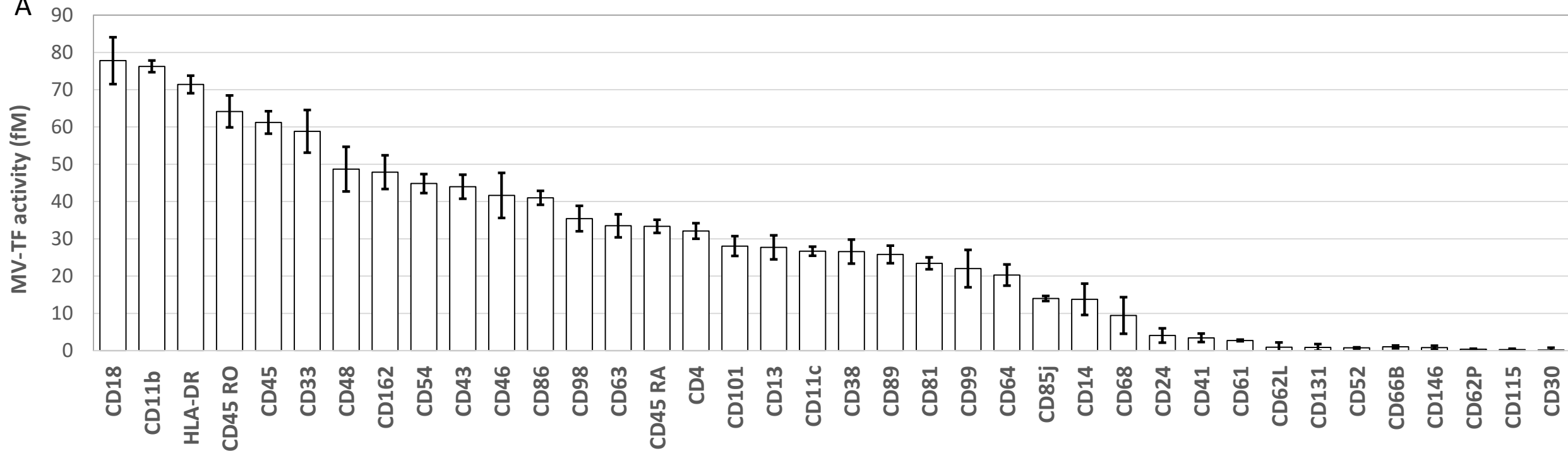
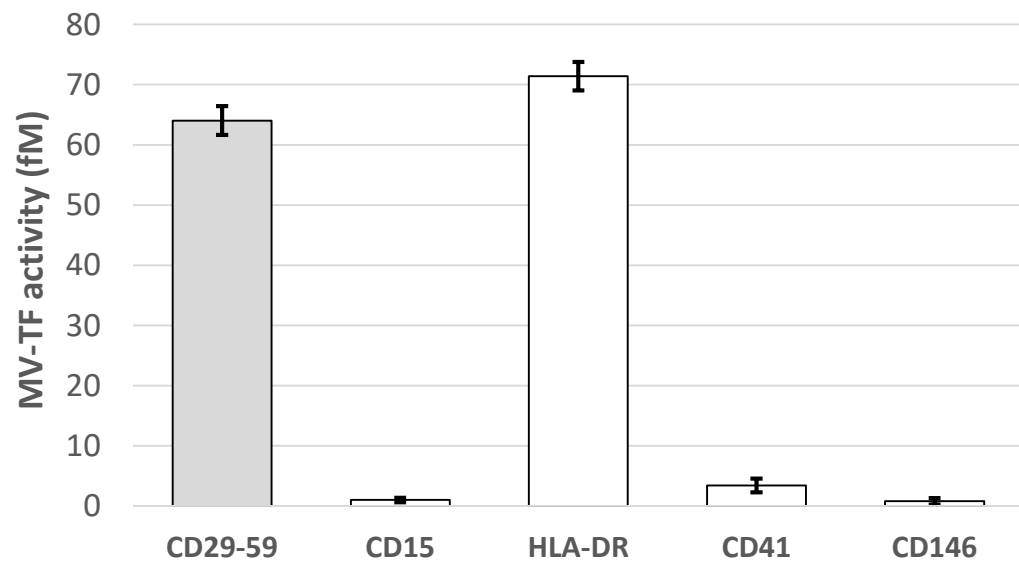
858









A**B****C**